Chemical Geology 635 (2023) 121623

Contents lists available at ScienceDirect

Chemical Geology

journal homepage: www.elsevier.com/locate/chemgeo

A grain-by-grain comparison of apatite fission-track analysis by LA-ICP-MS and the External Detector Method

Christian Seiler [a,1], Samuel C. Boone [a,b,*], Barry P. Kohn [a], Andrew J.W. Gleadow [a]

[a] School of Geography, Earth and Atmospheric Sciences, The University of Melbourne, Parkville 3010, Australia
[b] Department of Earth Sciences, University of Adelaide, Adelaide, SA 5005, Australia

ARTICLE INFO

Editor: Christian France-Lanord

Keywords:
Fission track
Apatite
External detector method
LA-ICP-MS
Model age

ABSTRACT

Laser-ablation inductively coupled plasma mass spectrometry (LA-ICP-MS) is increasingly used in fission-track analysis to determine the uranium content of host mineral specimens, particularly apatite. Fission-track dating by LA-ICP-MS (LAFT) has several advantages over the conventional External Detector Method (EDM), particularly in terms of sample turn-around times and the fact that neutron irradiations and the handling of radioactive materials are no longer necessary, while providing a similar level of in-situ information about parent nuclide (^{238}U) concentrations. In addition, it facilitates the simultaneous measurement of multiple isotopes for double or triple-dating approaches or compositional characterisation. While it is often implicitly assumed that the EDM and LAFT fission-track dating approaches produce equivalent results, this assertion has yet to be adequately tested. We present an extensive dataset of apatite fission track results from 17 samples representing a large range of fission-track ages (~0–2 Ga), ^{238}U concentrations (0.14–410 ppm) and thermal histories that were analysed grain-by-grain using both techniques in order to investigate whether they yield concordant results during routine fission-track analysis.

Apart from a few outliers, our data show that ^{238}U concentrations measured by the EDM and LAFT techniques yield indistinguishable results across at least three orders of magnitude when a similar calibration system against rapidly cooled standards (e.g., Durango) is used. Comparison of single grain pooled and central ages reveals that LAFT ages are within error of EDM ages for apatite fission track standards such as Fish Canyon Tuff or Durango, as well as for a range of other samples whose shorter mean confined track lengths (<13 μm) and broader track distributions indicate they experienced more complex cooling histories. The most important conclusion here is that both the conventional EDM and LAFT methods can be expected to yield identical results for the breadth of ages, ^{238}U concentrations, and underlying thermal histories commonly found in real world apatites.

Importantly, the aggregate empirical calibrations for EDM and LAFT mask an underlying assumption that the mean etchable range of fission fragments is a constant having the mean value observed for spontaneous tracks in age standards such as the Durango apatite. Given that this assumption is known to be false in the great majority of samples, it is our view that empirically derived EDM and LAFT fission-track ages are best considered as model ages and that there should be greater clarity about the assumptions involved in their calculation.

1. Introduction

Apatite fission-track analysis is one of the most widely applied thermochronometers to monitor the low-temperature evolution of the uppermost 3–5 km of the crust, with applications across a range of fields including tectonic and exhumation processes, landscape evolution, the history of sedimentary basins and sedimentary provenance studies (e.g. Gleadow et al., 2002; Wagner and Van Den Haute, 1992). The technique is based on the accumulation of radiation damage tracks (fission tracks) from spontaneous nuclear fission of ^{238}U in uranium-rich minerals such as apatite, zircon and titanite (e.g. Fleischer et al., 1975; Wagner and Van Den Haute, 1992). Like other radiometric dating techniques, the fission-track age is a function of the number of fission tracks ('daughter product') in a mineral grain, the ^{238}U concentration ('parent nuclide'),

* Corresponding author at: School of Geography, Earth and Atmospheric Sciences, The University of Melbourne, Parkville 3010, Australia.
E-mail addresses: christian.seiler@angloamerican.com (C. Seiler), samuel.boone@unimelb.edu.au (S.C. Boone), b.kohn@unimelb.edu.au (B.P. Kohn), gleadow@unimelb.edu.au (A.J.W. Gleadow).
[1] Present address: Anglo American, 201 Charlotte Street, Brisbane QLD 4000, Australia.

https://doi.org/10.1016/j.chemgeo.2023.121623
Received 27 March 2023; Received in revised form 5 June 2023; Accepted 4 July 2023
Available online 8 July 2023

and the total and spontaneous fission decay constants of ^{238}U. While measuring the number of fission tracks per unit area is relatively straightforward using optical microscopy, once they have been revealed by chemical etching (Fleischer and Price, 1964), measuring concentrations of ^{238}U at ppm levels and comparable spatial resolution has been more challenging.

In conventional fission-track analysis, ^{238}U concentrations are estimated indirectly by irradiating the sample with thermal neutrons in a nuclear reactor. Irradiation induces fission in a specific proportion of ^{235}U resulting in the formation of new 'induced' fission tracks. ^{238}U is then calculated using its virtually constant ratio to ^{235}U (Steiger and Jaeger, 1977). Induced fission tracks are usually monitored via a mica external detector placed adjacent to the polished grain mount during irradiation, a technique known as the External Detector Method (EDM; e.g., Gleadow, 1981). Mica detectors are then etched and induced tracks counted separately over the same region as spontaneous tracks (Gleadow, 1981). The number of induced tracks is then calibrated against standard glasses of known ^{238}U and ^{235}U concentration to estimate the ^{238}U content of grains being used to calculate the fission-track age.

This approach has several advantages that made the EDM the preferred technique for fission-track analysis over several decades. Firstly, by counting spontaneous and induced track densities over the exact same area, a separate fission-track age can be calculated for each analysed grain. Matching spontaneous and induced track densities also provides a solution to the problem of uranium zoning, which may occur in uranium-bearing minerals (e.g. Jolivet et al., 2003; Krishnaswami et al., 1974; Suzuki, 1988). In addition, the use of an empirical calibration factor (ζ) in the EDM technique allowed analysts to circumvent uncertainties in the decay constant for spontaneous fission, reactor efficiency and neutron dosimetry (Hurford, 1990; Hurford and Green, 1982; Hurford and Green, 1983). Despite its conceptual simplicity however, the EDM also has a number of disadvantages. Irradiation with thermal neutrons requires handling of radioactive materials, which is a safety hazard and greatly increases sample turn-around times, particularly if samples need to be sent across the globe to an appropriate reactor. Further, the number of reactors available for such thermal neutron irradiations is rapidly decreasing due to environmental, safety and political factors, thereby limiting options for future fission-track studies. Finally, the EDM technique is time consuming and tedious, requiring extensive empirical calibration and the counting of three separate track densities for each sample (spontaneous, induced and dosimeter).

With the development of high sensitivity, in situ mass spectrometry techniques such as laser-ablation inductively-coupled-plasma mass-spectrometry (LA-ICP-MS) in the 1990s, direct measurement of ppm-level concentrations of ^{238}U with high spatial resolution became a viable alternative to indirect measurement techniques such as the EDM. Building on the preliminary work of Cox et al. (2000) and Svojtka and Kosler (2002), Hasebe et al. (2004) developed the foundation for LA-ICP-MS based fission-track (LAFT) dating and presented a first comparison between the two techniques using three well-known apatite age standards. Encouraged by the results of this comparison, numerous studies have since published LAFT ages for apatite, zircon and volcanic glass (Boone et al., 2016; Boone et al., 2018; De Grave et al., 2012; Gleadow et al., 2015; Glorie et al., 2017; Hasebe et al., 2009; Hasebe et al., 2013; Ito and Hasebe, 2011; Li et al., 2016; Soares et al., 2014; Sueoka et al., 2012; Tian et al., 2014; Sun et al., 2021; McMillan et al., 2022). In recent work, Vermeesch (2017) developed a statistical basis for error propagation and the numerical issue of 'zero track' grains for LAFT dating.

LAFT dating has a number of clear advantages over the conventional EDM technique. Firstly, it avoids several of the disadvantages of EDM as outlined above (e.g., neutron irradiation) and provides significantly faster sample turn-around times. Secondly, LA-ICP-MS analysis allows virtually instantaneous measurement of many different isotopes (and trace element data), so that mineral grains can be dated using multiple geochronological systems simultaneously. Several studies have now reported results from LA-ICP-MS based 'double' or 'triple' dating to obtain U—Pb, fission track and (U—Th)/He ages simultaneously (e.g. Ansberque et al., 2021; Chew and Donelick, 2012; Chew et al., 2011; Danišík et al., 2010; Danišík, 2019; Evans et al., 2015; Hasebe et al., 2013; Noda et al., 2017; Reiners et al., 2007). A third major advantage is that it can potentially be used to measure the concentration of chlorine and other minor elements in apatite, which exert an important control on the annealing behaviour and are typically measured in a separate step using electron probe microanalysis (e.g. Green et al., 1986). Although analytically challenging due to a high first ionisation potential and high background signals, the work of Chew et al. (2013) has shown a convincing correlation between Cl concentrations measured by LA-ICP-MS and electron probe microanalysis, suggesting that direct measurement of Cl by LA-ICP-MS is a feasible alternative to electron probe microanalysis.

Theoretically, the use of LA-ICP-MS in fission-track dating could remove the need for an empirical ζ-calibration altogether, as the main components of a ζ-calibration are irradiation parameters, which are not applicable for LAFT, as well as the decay constant for spontaneous fission. While there was significant debate about the decay constant in the 1970s and 1980s, a review of the available measurements and underlying techniques led the IUPAC to recommend a value of $8.45 \pm 0.10 \times 10^{-17}$ a^{-1} (Holden and Hoffman, 2000), which is within error of more recent determinations (Guedes et al., 2003; Yoshioka et al., 2005). With the two principal arguments for ζ-calibration resolved, it is now possible to use LAFT analysis as an 'absolute' dating technique, i.e., one that is not dependent on independently constrained age standards. In practice, however, analysts still routinely employ an empirical LAFT approach, often referred to as a 'modified ζ-calibration'. However, given that this aggregate calibration factor incorporates a different set of constituent constants, we prefer a different designation, referred to here as a 'xi' (ξ) calibration, to clearly differentiate it from its EDM ζ-calibration counterpart (Chew and Donelick, 2012; Gleadow et al., 2015; Hasebe et al., 2013; Vermeesch, 2017).

Most studies using LAFT implicitly assume that their results are equivalent to the conventional EDM approach, yet this assumption has not been adequately tested. Results from the limited number of studies available have been encouraging, with absolute LAFT ages typically within error of published values (Gleadow et al., 2015; Hasebe et al., 2004; Hasebe et al., 2009; Soares et al., 2014). However, all of these studies were performed on well-known fission-track age standards, which are characterised by simple thermal histories marked by a single rapid cooling event, relatively young ages (<100 Ma), and a relatively homogeneous distribution of usually moderate ^{238}U concentrations (10–30 ppm for apatite).

In this study, we present the first comprehensive evaluation of grain-scale fission-track dating using the conventional ζ-calibrated EDM and empirical ξ-calibration LAFT dating approaches, based on a comparison of >570 single grain apatite fission-track ages from a total of 17 rock samples. The samples were chosen to cover a broad range of single grain ages (<1 Ma to >2 Ga), different thermal histories as recorded by fission-track length distributions, and ^{238}U concentrations that span several orders of magnitude (0.14–410 ppm) to provide a realistic assessment of how the two techniques compare under real-world conditions. The results show that LAFT dating yields results that are indistinguishable from EDM ages for samples across a wide range of ages, ^{238}U concentrations and underlying track length distributions.

2. Fission-track analysis

2.1. The Fission-Track Age Equation for the different methods

Fission tracks in apatite are ~16 μm long damage trails in the crystal lattice formed by the spontaneous fission of ^{238}U (Fleischer et al., 1975;

Wagner and Van Den Haute, 1992). Based on the fundamental age equation from radioactive decay, the number of spontaneous fission tracks in a given volume is given by:

$$N_s = \frac{\lambda_f}{\lambda}\left[^{238}U\right]\left(e^{\lambda t} - 1\right) \quad (1)$$

where N_s is the number of spontaneous fission tracks accumulated over time t, λ is the total decay constant of ^{238}U (principally alpha-decay), λ_f the fission decay constant of ^{238}U, and $[^{238}U]$ the current number of ^{238}U atoms per unit volume. The number of spontaneous fission tracks per unit volume is not measured directly but calculated from the areal track density ρ_s, which represents the total number of tracks per unit area that intersect a given grain surface:

$$N_s = \frac{\rho_s}{g_s R^{238} \eta q_s} \quad (2)$$

where g_s is a geometry factor that depends on the relationship of the counted surface to the fission events (ideally $g_s = 1$ for an internal sample grain surface, and 0.5 for external grain and external detector surfaces). R^{238} is the average etchable range of a spontaneous ^{238}U fission fragment and ηq is the detection efficiency, which is a combination of physical (η) and analyst-specific (q) factors that are difficult to disentangle (Fleischer et al., 1975; Jonckheere and Van den Haute, 2002). Applying eq. (2) in eq. (1) and solving for t leads to the age equation for absolute fission-track dating:

$$t = \frac{1}{\lambda} ln\left(1 + \frac{\lambda}{\lambda_f}\frac{\rho_s}{\left[^{238}U\right] g_s R^{238} \eta q_s}\right) \quad (3)$$

2.1.1. EDM age equation

In the EDM technique, $[^{238}U]$ is estimated by proxy using the number of induced tracks (N_i) implanted per unit volume via irradiation with thermal neutrons:

$$\left[^{238}U\right] = \frac{N_i}{I\sigma\Phi} \quad (4)$$

where I is the ^{238}U/^{235}U ratio, σ the cross-section of ^{235}U for fission induced by thermal neutrons and Φ the neutron fluence received in the nuclear reactor. The neutron fluence is difficult to measure directly and is estimated from the track density ρ_d counted in an external detector attached to a dosimeter glass of known ^{235}U concentration (e.g., CN, IRMM) using a proportionality factor B so that $\Phi = B\rho_d$. The number of induced tracks N_i is related to the track density ρ_i, measured per unit area of the mica external detector, via a modified form of Eq. (2). Substitution of Eqs. (2) and (4) in Eq. (3) yields the full age equation for the EDM:

$$t = \frac{1}{\lambda} ln\left(1 + \frac{\lambda}{\lambda_f}\frac{\rho_s}{\rho_i}\rho_d BI\sigma G\frac{R^{235}}{R^{238}}\eta q_{det}\right) \quad (5)$$

where $G = g_i/g_s = 0.5$ and ηq_{det} is the detection efficiency of the analyst for the detector. Fission fragment ranges of unannealed spontaneous and induced tracks are virtually equal in the same material (Bhandari et al., 1971; Togliatti, 1965) so that the ratio R^{235}/R^{238} was historically assumed to be 1, although this has long been known to be invalid in natural samples. In practice, the effect of differences between R^{235} and R^{238} is accounted for in ηq_{det} included in the ζ-factor, simplifying the age equation to:

$$t = \frac{1}{\lambda} ln\left(1 + \lambda\frac{\rho_s}{2\rho_i}\rho_d\zeta\right) \quad (6)$$

where ζ is a proportionality factor defined as:

$$\zeta = \frac{BI\sigma\eta q_{det}}{\lambda_f} \quad (7)$$

In principle the ζ-factor may be determined absolutely from its constituent constants but in practice it is determined empirically by rearranging eq. (6) and applying it to independently dated age standards that are analysed using identical analytical protocols using the formula:

$$\zeta = \frac{2\rho_i(e^{\lambda t} - 1)}{\lambda\rho_s\rho_d} \quad (8)$$

2.1.2. LAFT age equation

In the LAFT dating approach, the volume density of U-atoms $[^{238}U]$ is calculated from the ^{238}U concentration (in g.g^{-1}) measured by LA-ICP-MS (U) that is calibrated and corrected for fractionation and instrumental drift by analyses of an appropriate reference material with known ^{238}U and ^{43}Ca or ^{44}Ca concentrations for apatite:

$$\left[^{238}U\right] = \frac{N_A U D}{M^{238}} \quad (9)$$

where N_A is Avogadro's number, M^{238} the atomic weight of ^{238}U and D the density of the dated mineral. Combining eqs. (3) and (9) yields the age equation for absolute LAFT dating (Hasebe et al., 2004):

$$t = \frac{1}{\lambda} ln\left(1 + \frac{\lambda}{\lambda_f}\frac{\rho_s}{U}\frac{M^{238}}{N_A D R^{238}\eta q_s}\right) \quad (10)$$

where $g_s = 1$ for internal surfaces and has been removed in eq. (10). R^{238} is approximated by half the mean confined track length of spontaneous fission tracks, while ηq_s varies between 0.9 and 1.0 in apatite (Iwano and Danhara, 1998; Iwano et al., 1993; Jonckheere and Van den Haute, 2002; Soares et al., 2013). Following Hasebe et al. (2004, 2013), the aggregate constants in this equation may also be determined empirically against a set of age standards to give a factor ξ such that:

$$t = \frac{1}{\lambda} ln\left(1 + \lambda\frac{\rho_s}{U}\xi\right) \quad (11)$$

where

$$\xi = \frac{M^{238}}{\lambda_f N_A D R^{238}\eta q_s} \quad (12)$$

Importantly, in this case, there is only a single length term, R^{238}, the mean etchable range of spontaneous tracks.

Most studies using the LAFT method have determined ξ by employing an empirical calibration protocol against a set of age standards, the details of which vary slightly between laboratories (e.g., Hasebe et al., 2004, 2013; Cogné et al., 2020). An alternative empirical LAFT approach involves calculating ξ using published values for its constituent constants, with only the R^{238} value determined empirically against the underlying track distribution of an age standard. Gleadow et al. (2015), using a R^{238} value based on half the mean track length of the Durango apatite standard (7.17 μm), showed that both empirical LAFT approaches (i.e., with and without the use of published constant values) gave equivalent results for apatites from the Fish Canyon Tuff.

3. Experimental details

Fission track and LA-ICP-MS analyses were carried out at the University of Melbourne Thermochronology Laboratory. A total of 572 apatite grains from 17 samples were analysed using the empirical (ζ) EDM and (ξ) LAFT techniques. The samples were selected from published and unpublished sources to provide a spread of fission-track ages, ^{238}U concentrations and degrees of track annealing to compare the two techniques under real-world conditions. Analysed samples include Durango apatite and Fish Canyon Tuff, two widely used apatite fission-track age standards, a suite of seven basement samples from Mexico and Australia with simple track length distributions typical of undisturbed basement cooling, and a series of eight samples from Mexico as well as the Canadian and Fennoscandian shields, which record more complex

thermal histories, with fission-track ages ranging from Precambrian to Miocene. All samples are crystalline igneous or metamorphic rocks, comprised of grain populations assumed to have experienced a single thermal history with respect to the temperature sensitivity of the apatite fission track system. Further sample details including interpreted thermal histories and publication sources are provided in Table 1.

Samples were prepared following techniques described by Kohn et al. (2019). Following mineral separation, grains were mounted in epoxy, polished to expose internal grain surfaces and etched for 20 s at 20 °C using 5 M HNO_3. Muscovite external detectors were attached to each grain mount, packed into cans together with CN5 dosimeter glasses (Bellemans and De Corte, 1995) and irradiated in the former HIFAR reactor at the ANSTO Lucas Heights facility to a nominal neutron fluence of 1.6×10^{16} neutrons/cm^2. External detectors were etched in 48% HF for ~20 min at room temperature, affixed adjacent to the grain mount on a microscope slide and coated with a ~ 10 nm Au-film using a sputter coating unit to reduce internal reflections (Gleadow et al., 2009). Microscopy was carried out using a Zeiss Z1m microscope, at the time fitted with an Autoscan ES16 stage, and an AVT Oscar 3.3 MP CCD digital camera controlled by the in-house developed software *TrackWorks*. Slides were coordinated using three electron microscopy Cu grids glued to the mounts, and the grain mount and external detector aligned by matching apatite grains with their corresponding induced track prints on the mica. Grains suitable for analysis were identified using automated grain detection in *TrackWorks*, which uses circular polarised light to identify grains with the crystallographic *c*-axis parallel to the polished surface. Digital images were captured from the selected grain-mica pairs as vertical image stacks with a z-spacing of 0.5 μm in both transmitted and reflected light using a 100× dry objective. Spontaneous and induced tracks were counted automatically using the coincidence mapping algorithm of *FastTracks* (Gleadow et al., 2009, 2019) with manual review and editing as required.

Table 1
Samples analysed as part of the EDM-LAFT comparison.

Sample No.	Lithology	Locality	Interpreted thermal history	Source
A339	Granodiorite	Silvevaara, Finland	Complex (reheating)	Kohn et al. (2009)
BA06–011	Granodiorite	Sierra La Libertad, Mexico	Undisturbed basement cooling	Seiler (2009)
BA06–014	Granodiorite	Sierra La Libertad, Mexico	Undisturbed basement cooling	Seiler (2009)
BA06–016	Granodiorite	Sierra La Libertad, Mexico	Complex (reheating)	Seiler (2009)
BA06–017	Granodiorite	Sierra La Libertad, Mexico	Complex (reheating)	Seiler (2009)
BA06–018	Granodiorite	Sierra La Libertad, Mexico	Complex (reheating)	Seiler (2009)
BA06–019	Granodiorite	Sierra La Libertad, Mexico	Complex (reheating)	Seiler (2009)
BA06–020	Granodiorite	Sierra La Libertad, Mexico	Undisturbed basement cooling	Seiler (2009)
BA06–021	Granodiorite	Sierra La Libertad, Mexico	Undisturbed basement cooling	Seiler (2009)
BA06–027	Granodiorite	Sierra La Libertad, Mexico	Undisturbed basement cooling	Seiler (2009)
Dur-1	Durango apatite	Cerro de Mercado, Mexico	Rapid cooling	Gleadow et al. (1986a, 1986b)
FCT-1	Fish Canyon Tuff	Colorado, USA	Rapid cooling	Gleadow et al. (1986a, 1986b)
Har-1	Granodiorite	Harcourt, Australia	Undisturbed basement cooling	Gleadow and Lovering (1978)
SJ06–077	Tonalite	Sierra Juarez, Mexico	Undisturbed basement cooling	unpublished
SJC-1-2	Carbonatite	Siilinjarvi, Finland	Complex (multiple reheating)	unpublished
00ML10	Quartz gabbro	Sudbury, Canada	Complex (multiple reheating)	Lorencak et al. (2004)
00ML15	Norite	Sudbury, Canada	Complex (multiple reheating)	Lorencak et al. (2004)

Using spontaneous, induced and dosimeter track densities, an EDM fission-track age was calculated for each grain using eq. (6) with a total ^{238}U decay constant (λ) of 1.55123×10^{-10} a^{-1} (Jaffey et al., 1971) and a ζ-factor of 395 ± 18. The ζ-factor was calculated as the weighted mean of 18 calibration measurements for the same irradiation, etching and observation protocols using fission-track age standards Durango (31.4 ± 0.1 Ma; McDowell et al., 2005), Fish Canyon Tuff (28.4 ± 0.1 Ma; Gleadow et al., 2015) and Mt. Dromedary (98.5 ± 0.5 Ma; McDougall and Wellman, 2011). ^{238}U concentrations were indirectly calculated using the ratio of induced fission tracks and the known ^{238}U composition of the standard glass ($^{238}U_{sample} = \rho_i / \rho_d \times {}^{238}U_{standard}$). All errors are quoted at 1σ confidence levels unless otherwise stated. Sample mean EDM ages were then estimated as both pooled and central ages (Galbraith and Laslett, 1993).

^{238}U concentrations were also directly determined by LA-ICP-MS for the same apatite grains dated by EDM using a New Wave UP-213 Nd:YAG laser (λ = 213 nm) connected to an Agilent 7700× quadrupole ICP-MS (see Table 2 for operating parameters). To minimise grain loss during LA-ICP-MS due to laser-induced recoil and ejection, a thin veneer of superglue was applied to the mounts prior to laser ablation. A single spot with a diameter of 30 μm was ablated within the same area where spontaneous tracks were counted using a focused laser beam with a dwell time of 25 s, a pulse rate of 5 Hz and an energy density of 2.3 J/cm^2 at the target, resulting in ca. 16 μm deep ablation pits in apatite. Isotope measurements of ^{29}Si, ^{147}Sm, ^{232}Th and ^{238}U were made relative to ^{43}Ca using a NIST612 glass as a primary standard and tested using a series of secondary standards, including glasses NIST610 and NIST614, a polished Durango apatite crystal, and a powdered, homogenised and recrystallised apatite from the Mud Tank Carbonatite for which isotope concentrations were determined independently using solution ICP-MS. In sufficiently large grains, repeat single spot analyses was carried out on different portions of the counted area across different LA-ICP-MS sessions to evaluate the consistency of the ^{238}U results. Data reduction (corrections for instrument drift and signal blanks and all calibrations) was performed using the *Iolite* software package (Paton et al., 2011). Grains in which spontaneous track densities or LA-ICP-MS signals showed evidence for strong (>20–30%) ^{238}U zoning were rejected for further analysis due to the large uncertainties associated with unevenly distributed ^{238}U.

Single grain LAFT ages were calculated according to eqs. (11) using the same spontaneous track densities as for the EDM approach, a fission decay constant (λ_f) of 8.45 ± 0.10 × 10^{-17} a^{-1}; (Holden and Hoffman, 2000), a calculated apatite density (D) of 3.21 ± 0.04 g/cm^3 (Gleadow et al., 2015) and a detection efficiency factor (ηq_s) of 0.93 ± 0.01 (weighted mean of seven measurements from Iwano and Danhara, 1998; Jonckheere and Van den haute, 2002; Soares et al., 2013). The mean etchable range (R^{238}) was taken as half the mean spontaneous track length of Durango apatite (7.17 ± 0.83 μm) as determined from 470 length measurements made by Melbourne Thermochronology Group analysts using the same etching and measurement protocols. This, combined with the above constants, equates to a ξ-calibration of 2.185

Table 2
Summary of LA-ICP-MS operating conditions.

Laser	
Model	New Wave UP-213 Nd:YAG
Ablation cell	Supercell
Wavelength	213 nm
Pulse rate	5 Hz
Energy density	2.3 J/cm^2
Dwell time	25 s
Sampling scheme	Single/multiple spot
Spot size	30 μm
Pit depth	~16 μm
Primary standard	NIST612 (37.38 ± 0.08 ppm ^{238}U)
Secondary standards	NIST610
	NIST614
	Durango apatite
	Mud Tank (homogenised and recrystallised)

ICP-MS		
Instrument	Agilent 7700× quadrupole ICP-MS	
Forward power	1200 W	
Reflected power	1 W	
Sampling depth	7–8 mm	
Plasma gas flow (Ar)	15 l/min	
Carrier gas flow (Ar)	0.7–0.8 l/min	
Ablation gas flow (He)	0.4–0.5 l/min	
Data acquisition time	20 s	
Index isotope (integration time)	^{43}Ca	(25 ms)
Isotopes measured (integration time)	^{29}Si	(5 ms)
	^{147}Sm	(25 ms)
	^{232}Th	(40 ms)
	^{238}U	(40 ms)

$\pm 0.134 \times 10^{-3}$ Ma·cm^2. Confined fission-track lengths were determined on a second polished mount of each apatite that was exposed to a ^{252}Cf fission source prior to etching in order to enhance the number of confined tracks available for measurement (Donelick and Miller, 1991). Mean track lengths were averaged from refraction-corrected 3D lengths of ~100–120 confined fission tracks, measured in *FastTracks* using digital image stacks with a z-spacing of 0.3 μm. Sample mean LAFT ages were estimated as pooled ages following the equations of Hasebe et al. (2004). Central ages were calculated using the normal mixture modelling algorithm of Galbraith (2005) after logarithmic transformation of the single grain age data using the Newton-Raphson method (e.g. Kelley, 2003).

4. Results

Analysed samples show a wide range of fission-track densities, ^{238}U concentrations, single grain ages and track length distributions encompassing the natural variability that may be encountered during routine apatite fission-track analysis (Fig. 1). Spontaneous track densities vary over three orders of magnitude, from 'zero track' grains ($<3 \times 10^4$ cm^{-2}) to grains with a very large number of tracks that are challenging to count manually ($>1.5 \times 10^7$ cm^{-2}; Fig. 1a) with a mode of ~5×10^5 cm^{-2}. The corresponding ^{238}U concentrations as measured by LA-ICP-MS range from <0.2 ppm to >400 ppm, with values of 5–40 ppm being most prevalent (Fig. 1b). Apparent single grain ages determined by EDM range from <5 Ma to >3000 Ma, with most grains falling into one of three populations at ~1–100 Ma, ~200–600 Ma and ~800–2000 Ma (Fig. 1c) reflecting the thermal histories of the particular samples studied. Calculated EDM central ages vary over two orders of magnitude from 12 ± 1 Ma (BA06–018) to 1230 ± 73 Ma (SJC-1-2; Table 3). Cumulative confined track lengths show a negatively skewed, dominant peak at ~12–14 μm, with individual lengths measuring anywhere between ~1–17 μm (Fig. 1d). As expected, based on the samples' interpreted thermal histories, individual track length distributions are characterised by unimodal, skewed unimodal, bimodal or complex distributions (Gleadow et al., 1986b), with mean track lengths ranging from 9.9 to 14.8 μm and standard deviations of 0.8–3.9 μm (Table 3).

4.1. ^{238}U measurements

LA-ICP-MS analysis of ^{238}U concentrations in standard glasses NIST614 (0.823 ± 0.001 ppm), NIST612 (37.38 ± 0.04 ppm) and NIST610 (461.5 ± 0.6 ppm) indicates that measured ^{238}U concentrations reproduce the NIST-certified values (Reed, 1992a; Reed, 1992b; Reed, 1992c) across the entire range of ^{238}U concentrations investigated in this study (Fig. 2a). In all three standards, measured ~80 times across nine LA-ICP-MS sessions over a period of four months, the mean ^{238}U concentrations are within 1σ errors of the nominal ^{238}U values of these standards (Fig. 2a). Nonetheless, 23 out of a total of 240 single spot analyses (~10%) were outside 2σ confidence levels of the nominal value. The vast majority of these (21) were from the low-U standard NIST614, which also recorded the largest relative dispersion in ^{238}U measurements, suggesting that the sensitivity of the LA-ICP-MS system used is significantly reduced at low ^{238}U values of less than ~1 ppm. Reference ^{238}U concentration of in-house apatite standards Durango (12.2 ± 0.1 ppm) and sintered Mud Tank (3.00 ± 0.01 ppm) were determined by solution ICP-MS on a fragment of a single crystal cut by a precision diamond saw, with one half dissolved for solution ICP-MS analysis and the other half polished for LA-ICP-MS. The results show that the LA-ICP-MS measured mean ^{238}U concentration of Mud Tank (3.01 ± 0.05 ppm) is within 1σ error of its reference value (Fig. 2a), with about 10% (8 out of 83) of spot analyses falling outside 2σ of the nominal ^{238}U content. In Durango, a total of 9 out of 60 single spot analyses (~15%) were not within error of the nominal concentration defined by solution ICP-MS, although the mean ^{238}U content still lies within 2σ of the reference value (Fig. 2a).

A comparison of single grain ^{238}U concentrations measured by LA-ICP-MS against those indirectly calculated from EDM neutron induced tracks shows that the two techniques yield highly comparable ^{238}U estimates, with most values plotting close to the 1:1 correlation line (Fig. 2b). Importantly, there are no systematic trends towards either the low (<1 ppm) or high (>100 ppm) ends of the spectrum of analysed ^{238}U values, suggesting that the results are reliable across at least three orders of magnitude (Fig. 2b). Nevertheless, about 30% of individual measurements do not overlap within 2σ uncertainties, with ~15% of measurements not overlapping even at 3σ confidence levels.

Repeat analysis of 88 Durango fragments from a large single crystal across two different LA-ICP-MS sessions revealed that ^{238}U concentrations are largely consistent between different spots on the same grains, with only ~8% of repeat spots not within 2σ errors of the initial analysis and < 5% outliers that are outside 3σ confidence intervals (Fig. 3a). Even across larger Durango fragments, repeat ^{238}U measurements involving 4–14 analyses per grain showed that most single spot analyses are within error of the grain's mean ^{238}U content, with only two clear outliers outside the 2σ confidence intervals which may reflect natural intragrain ^{238}U zonation (Fig. 3c).

Triple analysis of two other samples (Har-1, SJC-1-2) with sufficiently large crystals for multiple spot analyses showed significantly more variation than Durango (Fig. 3b). Both these samples also show evidence of significant zoning based on the heterogeneous distribution of spontaneous tracks within grains. In Har-1, propagated analytical uncertainties are quite small so that ~50–60% of LA-ICP-MS single spot analyses fall outside 2σ of other measurements on the same grain, with ~30–50% even outside 3σ confidence intervals. However, such a large scatter is not entirely surprising given that 25% of the analysed grains show clear evidence for ^{238}U zoning with depth (included in Fig. 3b) and would therefore be rejected for routine LAFT dating. The results for SJC-1-2 are more encouraging, with only ~17–28% and ~ 11–15% of repeat analyses falling outside the 2σ and 3σ confidence intervals of other analyses on the same grain, respectively (Fig. 3b).

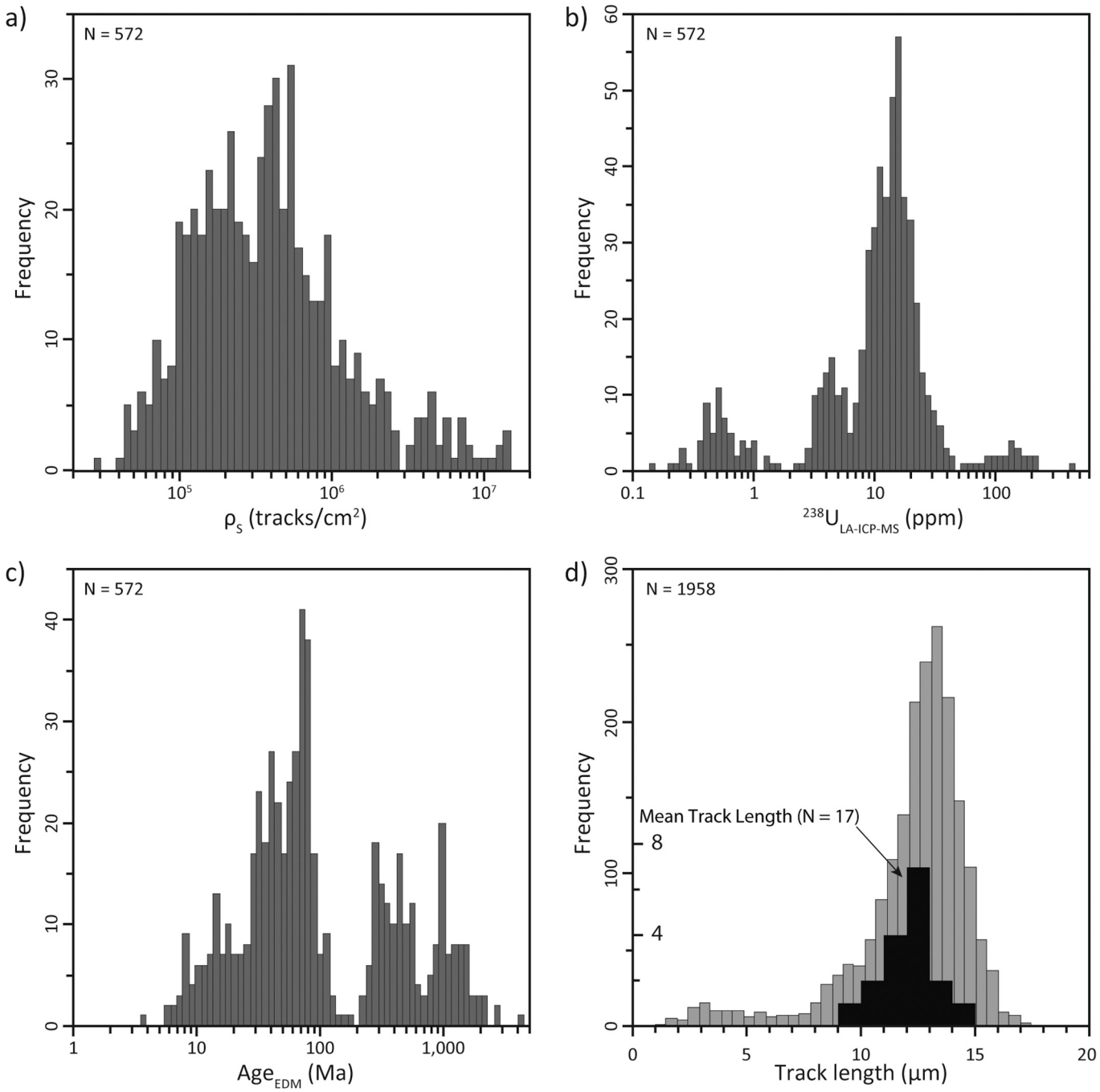

Fig. 1. Histogram distributions of single grain fission-track data from 17 samples selected to represent a wide range of fission-track densities, fission-track ages, uranium concentrations and thermal histories. a) Spontaneous fission-track densities; b) ^{238}U concentrations measured by LA-ICP-MS; c) conventional EDM single grain ages; d) individual (grey) and sample mean (black) track length distributions.

4.2. Fission-track age determinations

A comparison of apatite ages for fission-track standards Durango (Dur-1) and Fish Canyon Tuff (FCT-1) reveals that single grain ages derived by LAFT dating are statistically indistinguishable from those obtained using the conventional EDM technique. In both samples, all single grain LAFT ages are within error of the corresponding EDM ages. In FCT-1, the LAFT pooled age (29.0 ± 1.4 Ma) is within error of the EDM pooled age (28.1 ± 2.1 Ma) and published eruption ages for the Fish Canyon Tuff (~28 Ma; Gleadow et al., 2015; Hurford and Hammerschmidt, 1985; Phillips and Matchan, 2013) (Fig. 4a; Table 3). Calculated central ages of 31.7 ± 1.7 Ma (LAFT) and 28.0 ± 2.1 Ma (EDM) are also within 2σ error of each other and the eruption age (Table 3). In Durango, LAFT derived pooled (32.7 ± 0.8 Ma) and central (33.4 ± 1.0 Ma) ages are within error of the corresponding EDM pooled and central ages (33.1 ± 1.9 Ma), and within 2σ uncertainties of the 31.4 ± 0.1 Ma reference age of McDowell et al. (2005) (Fig. 4b; Table 3).

A similar comparison of single grain ages for all samples yields a strong correlation between the techniques across the entire analysed age spectrum (Fig. 5a). Of 572 grains analysed, only about 2% ($N = 12$) are not within 2σ uncertainties, with <1% ($N = 4$) clear outliers that are outside 3σ confidence intervals. Even upon closer inspection,

Table 3
Comparison of apatite fission track ages calculated by EDM and LA-ICP-MS methods.

Sample No.	No. of grains	Spontaneous track density ρ_s [10^5 cm^{-2}][a]	Induced track density ρ_i [10^5 cm^{-2}][a]	Dosimeter track density ρ_d [10^5 cm^{-2}][a]	External detector method				LA-ICP-MS method				Mean track length [μm ± se][a,c]		Standard deviation [μm]
					^{238}U [ppm ± 1σ][b]	Dispersion [%]	Pooled age [Ma ± 1σ]	Central age [Ma ± 1σ]	^{238}U [ppm ± 1σ]	Dispersion [%]	Pooled age [Ma ± 1σ]	Central age [Ma ± 1σ]			
A339	20	83.923 (9156)	24.592 (2683)	13.561 (5358)	24.6 ± 10.4	27	854.7 ± 44.8	848.8 ± 68.6	24.7 ± 12.7	26	760.7 ± 60.0	793.7 ± 49.0	10.84 ± 0.19	(158)	2.44
BA06–011	28	5.738 (984)	15.534 (2664)	10.471 (4486)	18.9 ± 5.0	18	75.9 ± 4.7	75.8 ± 5.4	18.6 ± 5.8	23	66.3 ± 3.9	67.4 ± 3.8	12.57 ± 0.15	(100)	1.49
BA06–014	26	3.978 (676)	13.188 (2241)	11.03 (4486)	15.2 ± 3.8	0	65.4 ± 4.3	65.4 ± 4.3	15.4 ± 4.4	0	58.1 ± 2.2	59.2 ± 2.4	12.19 ± 0.16	(124)	1.78
BA06–016	19	3.509 (380)	11.902 (1289)	11.403 (4486)	13.6 ± 4.7	0	66.1 ± 5.0	66.1 ± 5.0	13.8 ± 5.4	0	59.0 ± 3.9	59.8 ± 3.3	11.89 ± 0.33	(60)	2.56
BA06–017	25	4.359 (513)	15.031 (1769)	11.589 (4486)	16.9 ± 4.8	11	66.0 ± 4.6	65.8 ± 4.8	16.4 ± 5.1	22	61.6 ± 4.4	61.9 ± 4.2	11.91 ± 0.20	(137)	2.30
BA06–018	52	1.163 (335)	22.483 (6478)	11.776 (4486)	25.1 ± 10.3	7	12.0 ± 0.9	12.0 ± 0.9	22.7 ± 13.9	19	11.7 ± 0.8	12.4 ± 0.8	12.04 ± 0.23	(128)	2.58
BA06–019	24	3.693 (526)	11.044 (1573)	11.962 (4486)	24.2 ± 19.9	25	78.5 ± 5.5	71.1 ± 6.8	17.6 ± 25.7	21	68.4 ± 6.2	71.0 ± 5.2	12.20 ± 0.20	(98)	1.96
BA06–020	12	4.819 (400)	12.745 (1058)	9.116 (3150)	17.5 ± 3.1	8	67.7 ± 5.2	67.8 ± 5.4	16.8 ± 3.5	6	63.4 ± 4.2	64.7 ± 3.7	12.98 ± 0.20	(100)	2.00
BA06–021	19	4.793 (284)	12.473 (739)	9.431 (3400)	28.9 ± 17.3	27	71.2 ± 6.1	63.9 ± 7.4	31.2 ± 34.2	13	54.3 ± 4.4	58.7 ± 4.6	12.35 ± 0.17	(124)	1.94
BA06–027	19	4.528 (554)	13.912 (1702)	9.943 (3400)	17.8 ± 4.1	3	63.6 ± 4.4	63.6 ± 4.4	17.0 ± 5.0	19	58.9 ± 4.0	59.6 ± 3.8	11.74 ± 0.21	(100)	2.05
Dur-1	76	1.508 (1349)	12.445 (11133)	13.875 (4551)	11.2 ± 2.0	2	33.1 ± 1.9	33.1 ± 1.9	10.1 ± 1.7	0	32.7 ± 0.8	33.4 ± 1.0	13.89 ± 0.08	(120)	0.84
FCT-1	67	1.985 (360)	19.306 (3501)	13.881 (4595)	19.0 ± 6.2	16	28.1 ± 2.1	28.0 ± 2.1	15.2 ± 5.9	0	29.0 ± 1.4	31.7 ± 1.7	14.80 ± 0.08	(125)	0.90
Har-1	47	17.166 (8799)	16.441 (8427)	13.91 (4150)	15.1 ± 5.7	14	280.7 ± 14.2	278.1 ± 15.2	12.6 ± 5.2	13	288.5 ± 6.4	288.7 ± 6.7	12.72 ± 0.12	(146)	1.40
SJ06–077	20	43.284 (5349)	128.678 (15902)	10.331 (3206)	159.5 ± 62.2	10	68.3 ± 3.5	67.9 ± 3.8	153.4 ± 72.9	11	63.6 ± 1.9	64.0 ± 1.9	13.26 ± 0.09	(115)	1.01
SJC-1-2	63	3.158 (2378)	0.86 (648)	16.931 (11833)	0.8 ± 0.3	9	1233.0 ± 72.1	1230.0 ± 73.4	0.6 ± 0.2	13	1185.4 ± 47.5	1191.0 ± 38.7	11.62 ± 0.29	(111)	3.10
00ML10	30	7.618 (1981)	4.026 (1047)	11.23 (3470)	4.6 ± 1.1	1	406.6 ± 25.1	406.6 ± 25.2	3.6 ± 0.7	0	439.3 ± 11.7	441.5 ± 11.5	10.20 ± 0.35	(126)	3.94
00ML15	25	9.64 (2352)	4.23 (1032)	10.819 (5358)	4.9 ± 0.8	7	469.5 ± 28.4	470.2 ± 29.2	4.6 ± 0.6	5	453.4 ± 12.8	455.4 ± 12.4	9.93 ± 0.35	(123)	3.85

[a] Number of counts or measurements given in brackets.
[b] Weighted mean.
[c] se = standard error.

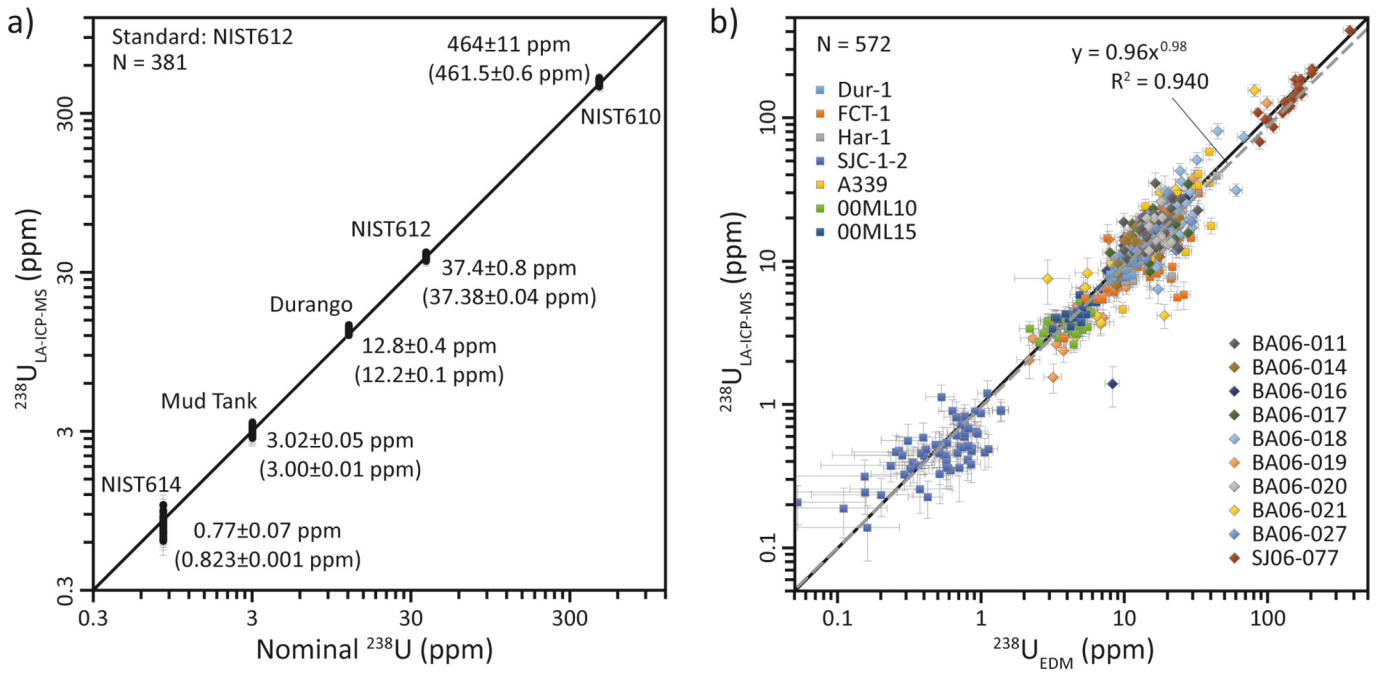

Fig. 2. *a) Comparison of ^{238}U concentrations measured in this study by LA-ICP-MS using NIST612 as a primary standard against published reference values for secondary standards (values in brackets), including standard glasses NIST610, NIST612, NIST614, a polished single crystal slice of Durango apatite and a homogenised and recrystallised Mud Tank apatite. See text for further details. b) ^{238}U concentrations measured by LA-ICP-MS and EDM based neutron dosimetry show that the two techniques yield compatible results. 1:1 identity line is shown as solid black line; grey dashed line represents a least squares power-law regression. Error bars are 1σ in this and subsequent figures.*

subdividing the results into groups of samples with similar thermal histories, single grain ages are closely clustered around the 1:1 identity line (Figs. 5 b-d), with regression lines showing no clear trends regardless of samples having undergone relatively simple (i.e., rapid cooling or undisturbed basement cooling) or more complex thermal histories, as defined in Table 1. Only the regression line through the combined single grain ages from rapidly cooled DUR-1 and FCT-1 apatites shows a significant deviation from the 1:1 line, an artefact of two outlier single grain ages from FCT-1 which are outside 3σ confidence intervals (Fig. 5b). When these outliers are removed, the regression line closely mirrors the 1:1 line (Fig. 5b).

The relationship of central and pooled ages between the two techniques is similar to that described for single grain ages (Fig. 6). LAFT derived pooled and central ages correlate very well with those obtained from EDM, with all samples within the 2σ confidence intervals of their respective EDM ages (Table 3). There does not appear to be any clear systematically offset between EDM and LAFT ages across the entire spectrum of ages in this dataset.

In Figs. 7-8, the four main parameters of the fission-track age equation (spontaneous track densities, induced track densities, ^{238}U concentration and fission-track length distributions) are plotted against the log ratio of single grain ages, which shows relative age differences between the two techniques irrespective of magnitude. The results show that neither spontaneous nor induced track densities have a significant influence on the EDM-LAFT single grain age ratio (Fig. 7a-b). Despite the fact that ^{238}U concentrations measured by LA-ICP-MS correlate well with those determined conventionally by EDM (Fig. 2b), a plot of the EDM-LAFT age ratio against measured ^{238}U values (Fig. 7c) shows a very weak correlation between older LAFT ages and lower ^{238}U values (Fig. 7c). If significant, this could indicate that either LA-ICP-MS ^{238}U measurements are slightly inaccurate at low and/or high uranium concentrations, or that there is a minor but systematic bias in the EDM ages. However, the performance of the LA-ICP-MS was monitored throughout this study using secondary standards that cover virtually the entire range of analysed ^{238}U concentrations (Fig. 2a), suggesting that LA-ICP-MS measured ^{238}U concentrations are accurate. Thus, the residual EDM-LAFT age difference, if indeed true, is more likely due to a small bias in the EDM ρ_i data, which we believe could be associated with analytical and statistical challenges associated with EDM analysis of low uranium, low track density grains. At track densities of $<1 \times 10^5$ cm^{-1} (e.g., SJC-1-2), there are <10 induced tracks in a typical area of 1×10^{-4} cm^2 used during fission-track analysis, which exacerbates uncertainties associated with grain-mica alignment and results in sampling sizes that could be insufficient for a full statistical representation of the stochastic decay process. This is consistent with observed intra-sample correlations between low induced track densities ($<5 \times 10^5$ cm^{-1}) and EDM-LAFT age ratios (Fig. 7b), which has to be an artefact of the EDM data given that a similar correlation is present even if densities are plotted directly against EDM single grain ages.

Irrespective of the exact cause for this minor residual uranium dependence, the results of Fig. 7 conclusively demonstrate that the EDM and LAFT techniques yield results that are generally indistinguishable.

In order to investigate the relationship between fission-track ages and track length distributions, mean track lengths and standard deviations are plotted against the logarithm of the EDM-LAFT age ratio (Fig. 8a and b, respectively). In both plots, there is no clear correlation between the age ratio and track length data, with all EDM and LAFT central ages being within two standard deviations of one another. This is consistent with the observed correlation between fission-track ages and thermal history groupings (Fig. 5).

5. Discussion

The key difference between fission-track dating using the conventional EDM technique and LA-ICP-MS analysis is the way in which present-day ^{238}U concentrations are measured. In the EDM technique, the ^{238}U content is estimated indirectly by relating the number of induced ^{235}U fission tracks to a dosimeter glass of known uranium concentration after irradiation by thermal neutrons. In LAFT, the ^{238}U content is measured directly using LA-ICP-MS analysis. A comparison of measured ^{238}U concentrations has shown that in general, the two techniques yield comparable results with no systematic trends across a

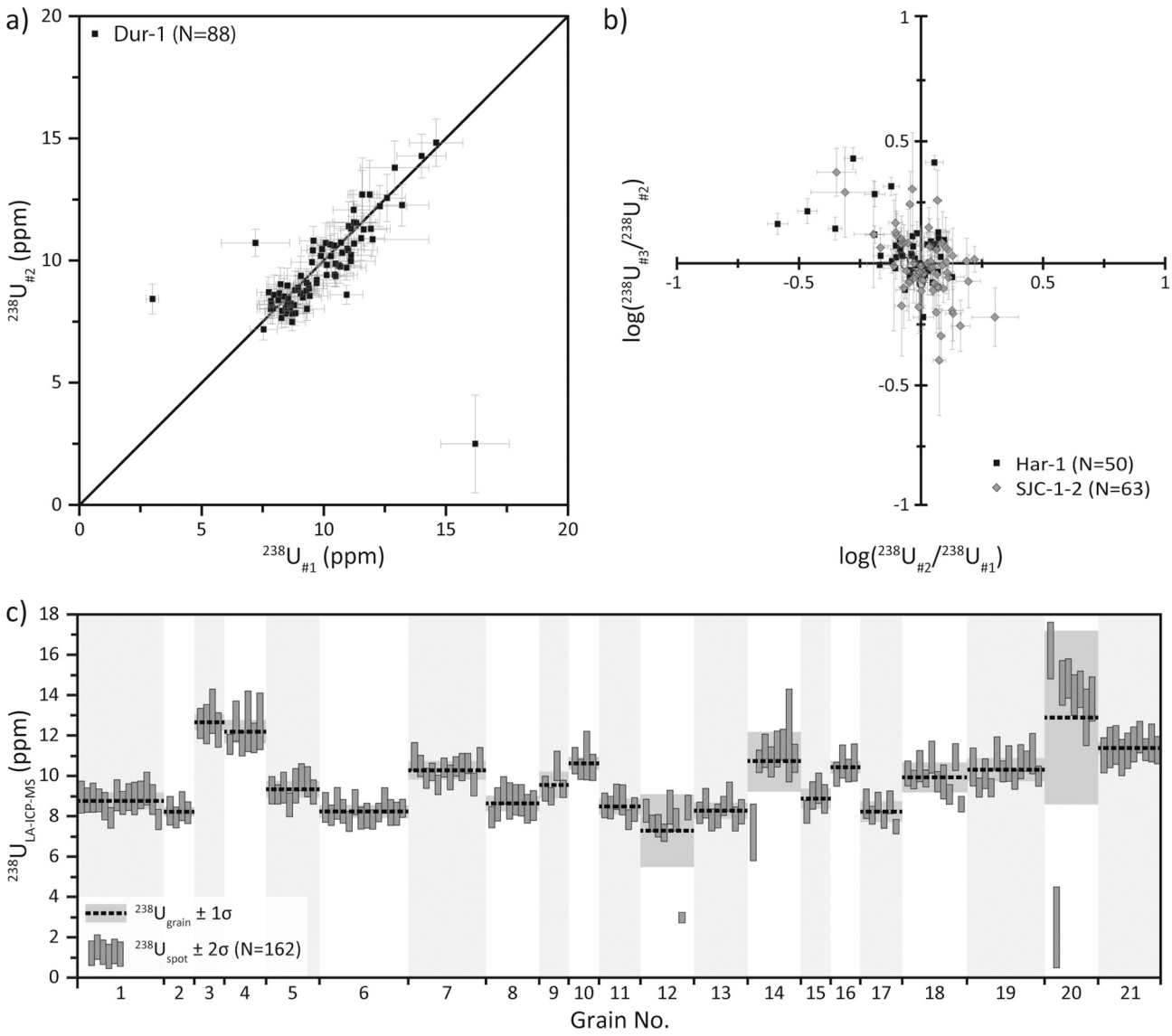

Fig. 3. Repeat ^{238}U measurements of apatite grains using multi-spot LA-ICP-MS analysis. a) Double analysis of Durango apatite grains (black line represents identity line). b) Triple analysis of apatite grains from samples Har-1 and SJC-1-2 on a log-log plot of ^{238}U ratios. c) Multi-spot analysis of ^{238}U (N = 4–14) for crystal fragments of Durango apatite. With the exception of two outliers, all analyses are within 2σ confidence intervals of the mean ^{238}U concentration for each grain. Note that mean uranium concentrations vary significantly between individual fragments of the same large crystal (7.3–12.9 ppm).

large spectrum of ^{238}U values, from <1 ppm to >400 ppm (Fig. 2b). The analysed range covers typical natural uranium concentrations in the vast majority of natural apatite samples, confirming that LA-ICP-MS is a feasible and accurate alternative to neutron irradiation for routine fission-track analysis, as previously assumed.

Despite these encouraging results, ^{238}U determinations at an individual grain level can differ significantly between the two techniques, with ~30% or ~ 15% of measurements falling outside the 2σ or 3σ confidence intervals of each other, respectively. This suggests that analytical errors underestimate the true uncertainties in some ^{238}U measurements, most likely due to an inhomogeneous distribution or 'zoning' of ^{238}U in apatite affecting the LA-ICP-MS measurements (Cogné and Gallagher, 2021). In the EDM technique, spontaneous and induced tracks are counted over the same area, so that the approach is generally considered to be insensitive to uranium zoning (e.g. Hurford and Green, 1982). While this is certainly true for lateral uranium zoning, it can only partially account for vertical uranium zoning, as half of the volume that contributed to spontaneous fission tracks on internal grain surfaces has been removed by polishing prior to neutron irradiation (Suzuki, 1988).

The same applies to LA-ICP-MS measurements, where vertical uranium zoning within apatite grains can be accounted for by weighting ^{238}U measurements inversely with depth (Chew and Donelick, 2012). However, lateral uranium zoning is significantly more challenging to address with LA-ICP-MS analysis than with EDM. One possible solution is to restrict spontaneous track counts to the exact area covered by the ablation pit, which by definition accounts for any lateral uranium variations across the analysed area. However, ablation pits are typically much smaller than the area available for counting, reducing the track count and therefore significantly increasing the uncertainty of the spontaneous track density and therefore the fission-track age. An alternative approach is to quantify lateral uranium zoning by measuring

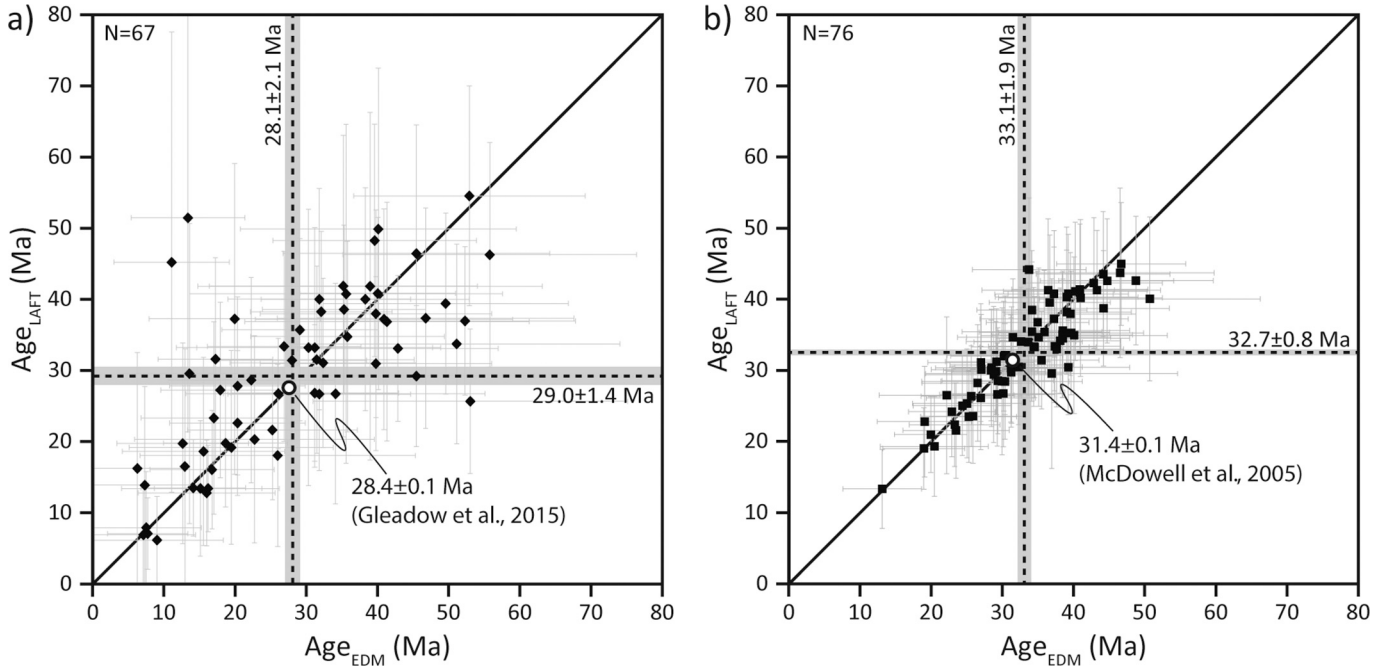

Fig. 4. Comparison of apatite fission-track ages for Fish Canyon Tuff (a) and Durango (b) apatite using the LAFT and EDM techniques. Both techniques yield largely consistent single grain ages, while pooled ages are statistically indistinguishable (e.g., within 1σ). Dashed orthogonal lines and grey bars represent pooled ages and errors. Open circles depict published reference ages; solid lines represent 1:1 unity.

multiple LA-ICP-MS spots for each grain (Cogné and Gallagher, 2021), ablating a transect across each grain, or scanning a raster pattern that covers the exact area counted or even the entire grain to generate a U map to characterize any zonation (e.g., Ansberque et al., 2021). Ablating multiple LA-ICP-MS spots is only feasible if grain sizes are sufficiently large to accommodate additional ablation pits, which is often not the case. Multiple ablation spots also significantly increase the likelihood of grain damage and loss during analysis which is counterproductive. In addition, running multiple spot analyses results in a multi-fold increase in LA-ICP-MS analysis time and cost. Using a scanning ablation mode may thus be preferable, although in this case the signal is a function of both lateral and vertical uranium distributions, making it difficult to differentiate and correct for vertical uranium zoning. In addition, there are several practical considerations that are yet to be addressed, including the question of whether matrix variations and possible isotope diffusion near earlier ablation sites have any adverse effects on ^{238}U measurements. For the present study, a much simpler option was adopted, whereby grains showing any evidence for lateral or vertical uranium zoning (recorded by variation in spontaneous track densities or LA-ICP-MS signals respectively) are rejected. We have found this to be a practical solution that has worked well for many hundreds of samples where it could safely be assumed that all constituent apatite grains have shared the same thermal history relative to the fission track system. However, this may not be appropriate for detrital studies where the removal of U-zoned grains may remove important detrital source populations comprised entirely of crystals with heterogenous compositions (Rolland et al., 2019) and consequently bias results. In those cases, restricting fission track counting to the exact area of the ablation pit or performing LA-ICP-MS rastering may be more suitable. Yet, the analysis of compositionally zoned apatites unavoidably introduces greater doubt regarding the assumption that the U-distribution of the removed portion of polished grains mirrors that of the preserved, analysed crystal fragments.

Despite the fact that individual grain ^{238}U determinations are not always within error, our results have clearly shown that in general, ^{238}U concentrations measured by LA-ICP-MS are consistent with those obtained by EDM. As expected, given that the single grain fission-track ages reported here are based on identical spontaneous track counts and comparable ^{238}U concentrations, EDM and LAFT derived ages are in general statistically indistinguishable.

5.1. *Future considerations about the interpretation of fission-track ages*

On geological time scales, fission tracks in apatite are relatively stable at ambient temperatures but anneal progressively at temperatures above ~60 °C, with virtually instantaneous fading above ~110 °C (Gleadow and Duddy, 1981). Track annealing results in a gradual shortening of the etchable fission-track length, which reduces the probability of a track intersecting the internal surface and thus decreasing the apparent fission-track age (Green, 1988; Wagner, 1979). As a result, fission-track ages are normally interpreted together with their corresponding track length distributions (Gleadow et al., 1986b), which can then be used to reconstruct the thermal history of a sample using numerical annealing algorithms (e.g. Ketcham et al., 2007; Laslett et al., 1987).

When using the empirical calibration approach, for either the EDM or LAFT methods (see (7) and (12) above), the mean spontaneous track length R^{238} is implicitly assumed to be constant for all unknowns, with a value equivalent to the mean etchable track range in the age standard materials used to make the calibration. However, it has long been known that R^{238} is in fact a variable showing a substantial range of values from sample to sample (e.g., Gleadow et al., 1986a, 1986b). This reality is mostly hidden from view by the use of the aggregate ζ- or ξ-constants, and in the case of the EDM, by the long-obsolete assumption that the

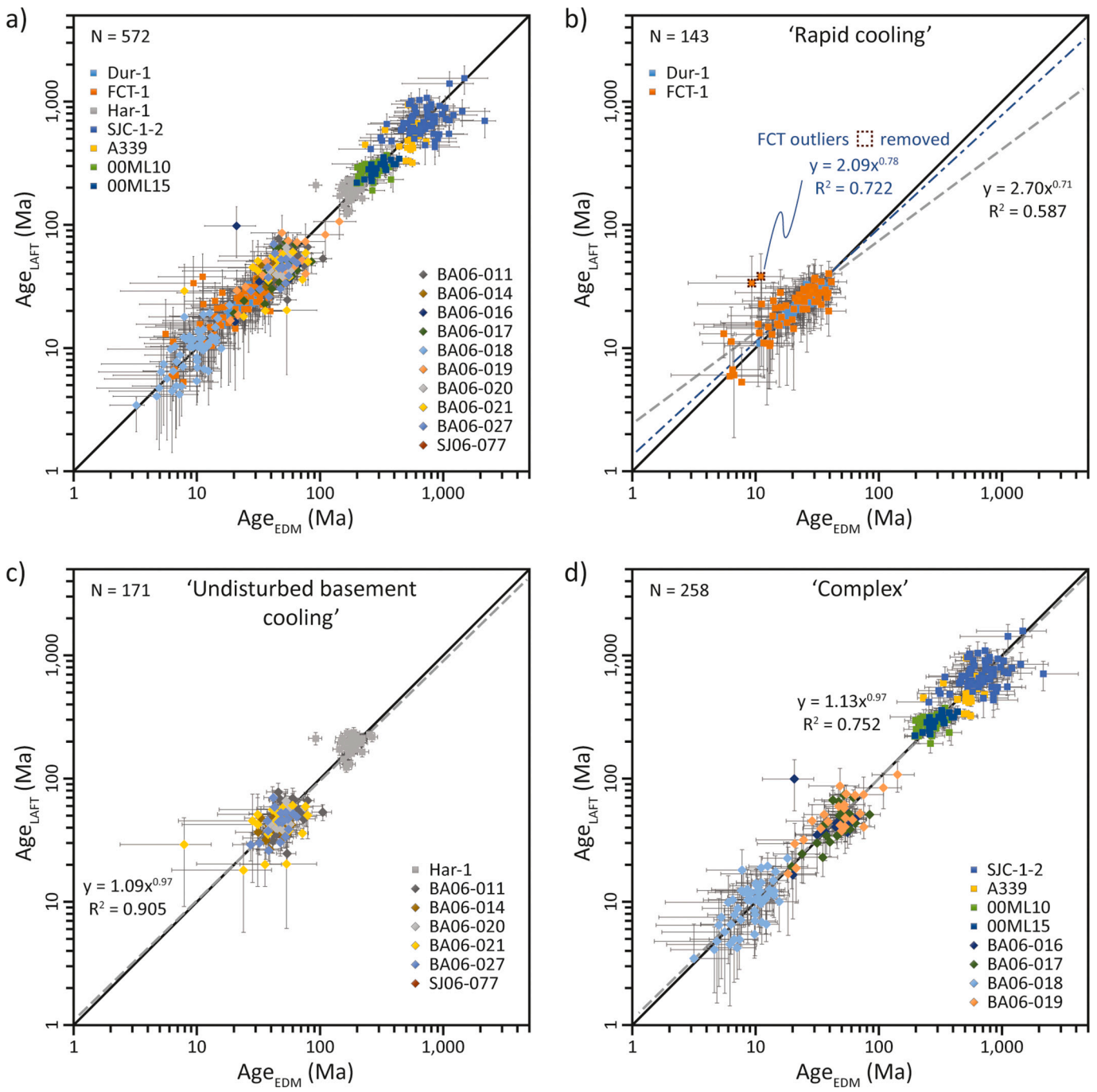

Fig. 5. a) Comparison of apatite single grain ages for all 17 samples using the LAFT and EDM techniques. b-d) Results subdivided according to the interpreted thermal histories of samples (Table 1). LAFT and EDM ages are indistinguishable for rocks that experienced rapid cooling (b), undisturbed basement cooling (c) or complex cooling histories (d). Grey dashed lines represent least squares regressions; 1:1 unity is shown as black solid lines.

lengths of spontaneous and induced tracks are equivalent and cancel out.

It is therefore appropriate to consider what fission-track ages mean when calculated with the implicit assumption of a constant value for R^{238}, which is the case for almost all fission track age determinations regardless of the method used. The question of whether conventional fission track ages should be corrected for length reduction using an appropriate ratio R_{ζ}^{238}/R^{238} (eqs. 11 and 12), or whether absolute LAFT ages should be calculated as 'model' ages using a constant range factor R_{ζ}^{238} is beyond the scope of this paper. Such a decision cannot be made unilaterally by a single laboratory but needs to be discussed and agreed upon by the entire fission track community. In the interest of inter-laboratory consistency and data continuity, we propose that until broad consensus is achieved, conventional fission-track ages are best considered as model ages and that there should be greater clarity about the assumptions involved in their calculation. Such fission-track model ages can be understood as the fission-track age that would be obtained if the sample had the same track length distribution as the age standards used in calibration.

5.2. *A comment on parameters of the LAFT age equation*

Apart from fission-track lengths, there are several other parameters that are not in the conventional EDM age equation, which could

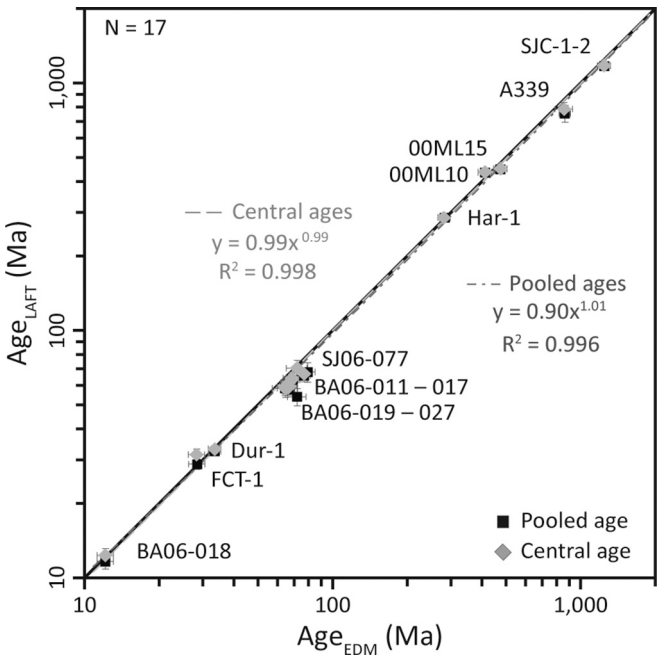

Fig. 6. Compilation of pooled and central ages calculated using the LAFT and EDM techniques. A least squares regression (grey dashed line) shows an excellent correspondence between results produced by the two techniques.

influence LAFT ages. Some of these are fixed physical properties that are either well defined (Avogadro's number, atomic weight of ^{238}U) or would introduce a consistent offset in LAFT ages (e.g., fission decay constant), for which there is no evidence in our data. Other parameters such as apatite density, detection efficiency and matrix properties differ between individual samples and/or grains as a result of compositional variations or thermal histories. Although a detailed analysis of these requires further research that is beyond the scope of this paper, there are some preliminary observations that are worth mentioning here.

The apatite density D adopted in this study (3.21 g/cm^3) was calculated for Fish Canyon Tuff by Gleadow et al. (2015) based on analyses and unit cell dimensions of Carlson et al. (1999). Although apatite density can vary between ~3.10–3.35 g/cm^3 (Deer et al., 1992), most Cl-, F- and OH-apatites seem to fall into a much narrow interval of ~3.17–3.29 g/cm^3 as calculated for different apatite varieties based on the compositional data of Barbarand et al. (2003) and (Carlson et al., 1999). Applying these densities to the LAFT age equation (eq. 10) would reduce single grain ages by up to ~2.1% (D = 3.29 g/cm^3) or increase ages by ~1.5% (D = 3.17 g/cm^3). Even if the full range of densities reported by Deer et al. (1992) is considered, LAFT ages would only vary by about ±4%, which is smaller than the typical uncertainty of fission-track ages. In an ideal situation, each single grain age would be based on the actual apatite density of the analysed grain, which would probably have to be calculated from compositional data acquired using electron microprobe analysis or major element LA-ICP-MS. Given that the associated errors are comparatively small, however, a more practical approach may be to use empirical relationships between apatite density and anion concentrations as suggested by Gleadow et al. (2015).

The detection efficiency ηq_s represents the fraction of fission tracks intersecting an observation surface that are revealed and counted using laboratory-specific etching and observation protocols. The limited number of existing estimates of ηq_s for apatite surfaces parallel to the c-axis range between 0.90 and 0.95 (Iwano and Danhara, 1998; Iwano et al., 1993; Jonckheere and Van den Haute, 2002; Soares et al., 2013) with a weighted mean of 0.93 ± 0.01 as used in this study. Adopting a lower (0.90) or higher (0.95) value for ηq_s would increase or decrease ages by approximately 3.5% and 2.1%, respectively. However, the detection efficiency is not a fixed parameter but decreases with shorter track lengths (Jonckheere and Van den Haute, 2002), which could account for up to 5% of the reported systematic age discrepancy between LAFT and EDM ages at shorter track lengths. It is worth noting that only a limited number of apatite compositions have been analysed for their ηq_s values so far. It is therefore possible that future determinations of the detection efficiency using different apatite samples may fall outside the range 0.90–0.95, which would add to any bias in fission track ages. This is undoubtedly an area that requires more research as LAFT dating gains in popularity.

Another potential uncertainty for LAFT dating is whether variations in the matrix properties of different apatite crystals and LA-ICP-MS standards could have an adverse effect on ^{238}U measurements. Different geochemical, mineralogical and laser properties ("matrix effects") can change the ablation and ionisation efficiency during LA-ICP-MS, which is known to result in element fractionation (Guillong and Günther, 2002; Jochum et al., 2007; Morrison et al., 1995). Because isotope concentrations are not measured directly from the signal but relative to an internal standard of assumed stoichiometric abundance such as ^{43}Ca, any change in isotope ratios (e.g., ^{238}U/^{43}Ca) due to element fractionation between different materials or mineral compositions also affects the measured concentration of the isotope, in this case ^{238}U. In order to avoid matrix effects, LA-ICP-MS analyses would ideally be calibrated against standards of similar physical and chemical composition. While some candidates were proposed as potential matrix-matched standards for apatite LA-ICP-MS analysis (e.g. Durango, Mud Tank; Soares et al., 2015), detailed investigations revealed significant heterogeneities in ^{238}U concentrations within individual apatite crystals of these samples (e.g. Boyce and Hodges, 2005). Although such heterogeneities can potentially be avoided by careful pre-screening of natural crystals (Chew et al., 2016) or mechanical homogenisation and sintering (Chung et al., 2016), more data from different laboratories is needed to demonstrate if matrix-matched standards are sufficiently homogeneous for routine use as primary LA-ICP-MS standards.

In our analysis, LA-ICP-MS results are calibrated using reference glass NIST612 as a primary standard and using a Durango crystal and sintered Mud Tank apatite as matrix-matched secondary standards to monitor the performance of the LA-ICP-MS analyses. The results have shown that although between 10 and 15% of individual LA-ICP-MS measurements do not fall within error of the reference value, mean ^{238}U concentrations are concordant with the corresponding solution ICP-MS concentrations. This suggests that although a matrix-matched standard would undoubtedly be preferable, there does not appear to be a systematic matrix bias when using NIST glass as a standard for apatite LA-ICP-MS analysis, at least not at the precision required for LAFT dating. In addition, the lack of a correlation between fission-track ages and spontaneous fission-track density (Fig. 7a) suggests that unlike zircon (Allen and Campbell, 2012), radiation damage does not appear to result in significant element fractionation in apatite.

6. Conclusions

A comprehensive grain-by-grain comparison of apatite fission-track data obtained by LA-ICP-MS and the conventional EDM technique shows that the two approaches produce statistically indistinguishable results when based on similar empirical calibrations. In other words, the EDM and LAFT fission track techniques produce comparable ages when

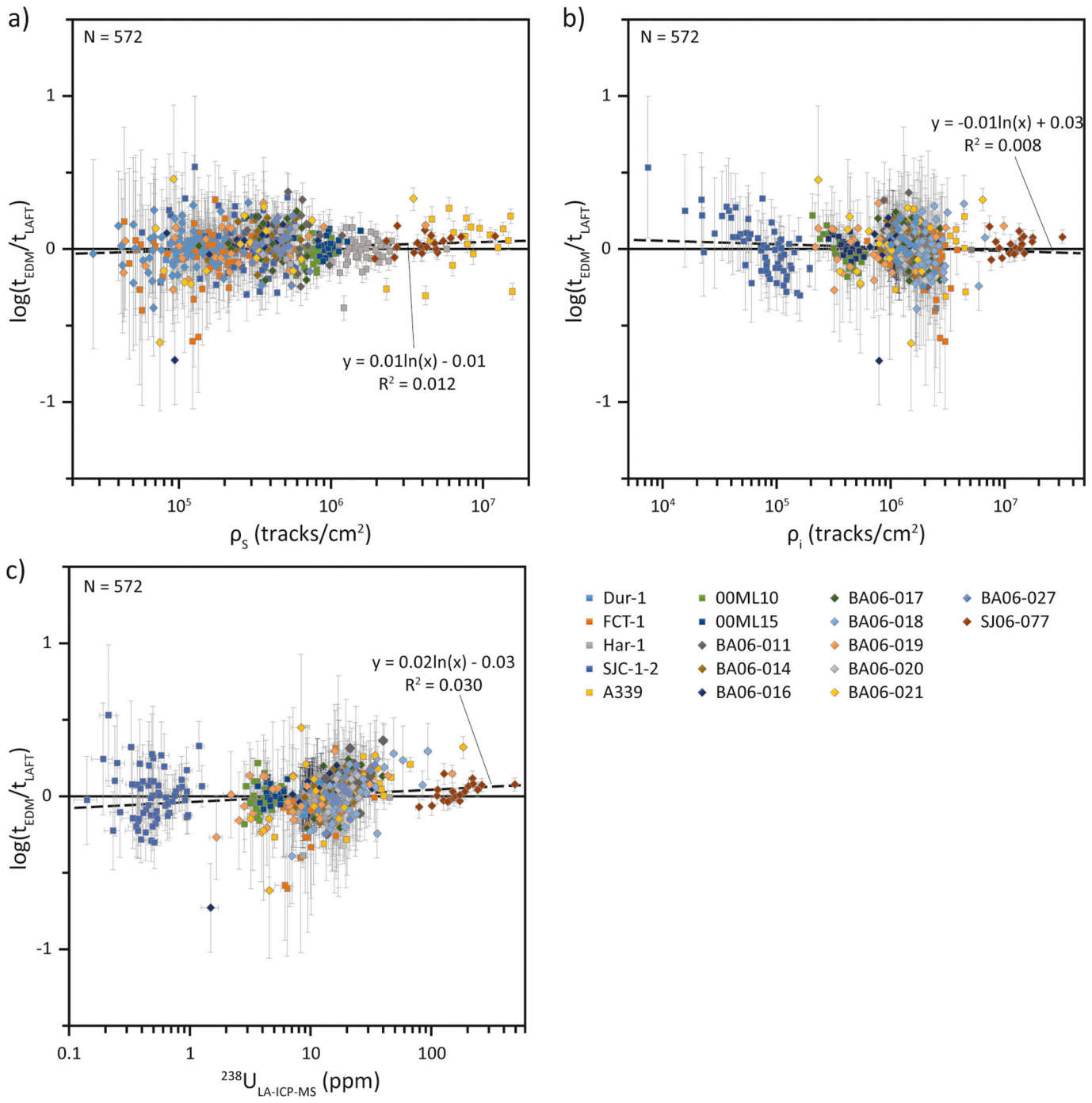

Fig. 7. Age difference shown as the logarithmic ratio between EDM and LAFT single grain ages as a function of spontaneous track density (a), induced track density (b) and LA-ICP-MS measured ^{238}U concentrations (c). Dashed lines show least squares logarithmic regressions. There is no clear correlation between age difference and either spontaneous or induced track density. LA-ICP-MS measured ^{238}U values show a slight trend towards older LAFT ages at low uranium values.

calibrated against similar rapidly cooled standards with long mean track lengths (~14.5 μm). This was true across a total of 572 grains from 17 samples that were analysed to represent a wide range of fission-track ages, track densities, uranium concentrations and thermal histories.

The aggregate empirical calibrations mask an underlying assumption that the mean etchable range of fission fragments is a constant having the mean value observed for spontaneous tracks in age standards such as the Durango apatite. Given that this assumption is known to be false in the great majority of samples, we suggest that fission track ages calculated in this way be understood as model ages in order to make this clear.

Measured ^{238}U concentrations yield consistent results by the two methods with no systematic trends across three orders of magnitude (<1 ppm to >400 ppm), although up 10% of individual analyses fall outside 2σ confidence levels. Multiple LA-ICP-MS spot analyses of individual grains show that while the results are consistent for grains with relatively homogeneous uranium distributions (e.g., Durango), measurements can be significantly different when uranium distributions are heterogeneous, implying that internal errors of LA-ICP-MS measurements are insufficient to account for the natural variability of uranium concentration.

A comparison of single grain pooled and central ages between the two techniques shows that fission-track ages are statistically

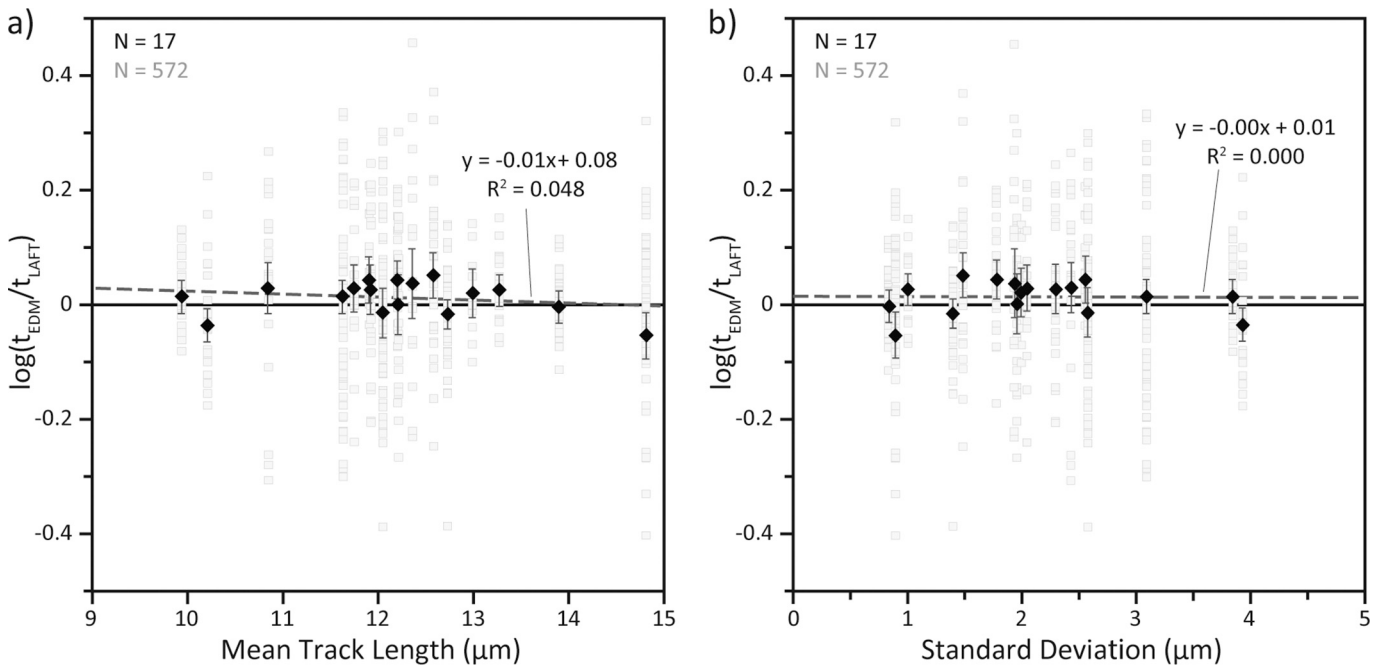

Fig. 8. EDM-LAFT age difference shown as a function of mean track length (a) and standard deviations (b). Grey dots indicate single grain ages; black diamonds and lines represent central ages and associated errors. The plots show that both the LAFT and EDM techniques yield comparable fission-track ages across the range of mean track lengths and standard deviations.

indistinguishable, regardless of how simple or complex the thermal history may be for a particular sample. Other parameters, such as spontaneous or induced track densities and uranium concentrations, also do not have a significant effect on fission track ages.

Declaration of Competing Interest

Melbourne Thermochronology Laboratory under Andrew Gleadow & Barry Kohn reports financial support was provided by Australian Research Council. Melbourne Thermochronology Laboratory under Andrew Gleadow & Barry Kohn reports financial support was provided by AuScope.

Data availability

All detailed data used in this study are presented in Tables 1, 2, 3 and A.1

Acknowledgements

The authors would like to thank Ling Chung and Abaz Alimanovic for technical support during fission track dating and LA-ICP-MS analysis. Alan Greig is thanked for the solution ICP-MS data and for helpful discussions regarding LA-ICP-MS analysis. Pieter Vermeesch helped with the equations for central age calculations using the normal mixture-modelling algorithm. The automated fission track analysis facility at the University of Melbourne was developed with support from Australian Research Council Grants LP0348767 and LE0882818 and additional operational and equipment funding from the National Collaborative Research Infrastructure Strategy (NCRIS) AuScope program (https://www.auscope.org.au/) and the Education Investment Fund AGOS programs. The Melbourne Thermochronology Laboratories operate under the University of Melbourne TrACEES Research Platform.

Appendix A. Supplementary data

Supplementary data to this article can be found online at https://doi.org/10.1016/j.chemgeo.2023.121623.

References

Allen, C.M., Campbell, I.H., 2012. Identification and elimination of a matrix-induced systematic error in LA–ICP–MS 206 Pb/238 U dating of zircon. Chem. Geol. 332, 157–165.
Ansberque, C., Chew, D.M., Drost, K., 2021. Apatite fission-track dating by LA-Q-ICP-MS imaging. Chem. Geol. 560, 119977.
Barbarand, J., Carter, A., Wood, I., Hurford, T., 2003. Compositional and structural control of fission-track annealing in apatite. Chem. Geol. 198 (1–2), 107–137.
Bellemans, F., De Corte, F., Van den Haute, P., 1995. Composition of SRM and CN U-doped glasses: significance for their use as thermal neutron monitors in fission track dating. Radiat. Meas. 24, 153–160.
Bhandari, N., et al., 1971. Fission fragment tracks in apatite: Recordable track lengths. Earth Planet. Sci. Lett. 13 (1), 191–199.
Boone, S., Seiler, C., Reid, A., Kohn, B., Gleadow, A., 2016. An Upper cretaceous paleo-aquifer system in the Eromanga Basin of the Central Gawler Craton, South Australia: evidence from apatite fission track thermochronology. Aust. J. Earth Sci. 63 (3), 315–331.
Boone, S.C., et al., 2018. Influence of Rift Superposition on Lithospheric Response to East African Rift System Extension: Lapur Range, Turkana, Kenya. Tectonics 37 (1), 182–207.
Boyce, J., Hodges, K., 2005. U and Th zoning in Cerro de Mercado (Durango, Mexico) fluorapatite: Insights regarding the impact of recoil redistribution of radiogenic ^{4}He on (U–Th)/he thermochronology. Chem. Geol. 219 (1–4), 261–274.
Carlson, W.D., Donelick, R.A., Ketcham, R.A., 1999. Variability of apatite fission-track annealing kinetics: I. Experimental results. Am. Mineral. 84 (9), 1213–1223.
Chew, D.M., Donelick, R.A., 2012. Combined apatite fission track and U-Pb dating by LA-ICP-MS and its application in apatite provenance analysis. Quantitative mineralogy and microanalysis of sediments and sedimentary rocks. Miner. Assoc. Can. Short Course 42, 219–247.
Chew, D.M., Sylvester, P.J., Tubrett, M.N., 2011. U–Pb and Th–Pb dating of apatite by LA-ICPMS. Chem. Geol. 280 (1–2), 200–216.
Chew, D.M., Donelick, R.A., Donelick, M.B., Kamber, B.S., Stock, M.J., 2013. Apatite Chlorine Concentration Measurements by LA-ICP-MS. Geostand. Geoanal. Res. 38 (1), 23–35.
Chew, D.M., et al., 2016. (LA, Q)-ICPMS trace-element analyses of Durango and McClure Mountain apatite and implications for making natural LA-ICPMS mineral standards. Chem. Geol. 435, 35–48.
Chung, L., Kohn, B.P., Gleadow, A.J.W., Greig, A., 2016. The potential of using sintered Mud Tank apatite as a matrix-matched uranium reference material for AFT LA-ICP-MS dating. In: 15th International Conference on Thermochronology, Maresias, Brazil, pp. 62–63.
Cogné, N., Gallagher, K., 2021. Some comments on the effect of uranium zonation on fission track dating by LA-ICP-MS. Chem. Geol. 573, 120226.
Cogné, N., Chew, D.M., Donelick, R.A., Ansberque, C., 2020. LA-ICP-MS apatite fission track dating: A practical zeta-based approach. Chem. Geol. 531, 119302.

Cox, R., Kosler, J., Sylvester, P., Hodych, J., 2000. Apatite fission-track (FT) dating by LAM-ICO-MS analysis, Goldschmidt. J. Conf. Abstract. 322.
Danišík, M., 2019. Integration of fission-track thermochronology with other geochronologic methods on single crystals. In: Malusà, M., Fitzgerald, P. (Eds.), Fission-Track Thermochronology and its Application to Geology, Springer Textbooks in Earth Sciences, Geography and Environment. Springer, Cham, pp. 93–108.
Danišík, M., et al., 2010. Tectonothermal history of the Schwarzwald Ore District (Germany): an apatite triple dating approach. Chem. Geol. 278 (1–2), 58–69.
De Grave, J., et al., 2012. Late Palaeozoic and Meso-Cenozoic tectonic evolution of the southern Kyrgyz Tien Shan: Constraints from multi-method thermochronology in the Trans-Alai, Turkestan-Alai segment and the southeastern Ferghana Basin. J. Asian Earth Sci. 44, 149–168.
Deer, W.A., Howie, R.A., Zussman, J., 1992. An Introduction to the Rock-Forming Minerals. Longman.
Donelick, R.A., Miller, D.S., 1991. Enhanced TINT fission track densities in low spontaneous track density apatites using ^{252}Cf-derived fission fragment tracks: A model and experimental observations. Nuclear Tracks Radiation Measure. 18 (3), 301–307.
Evans, N., et al., 2015. An in situ technique for (U–Th–Sm)/He and U–Pb double dating. J. Anal. At. Spectrom. 30 (7), 1636–1645.
Fleischer, R.L., Price, P.B., 1964. Techniques for geological dating of minerals by chemical etching of fission fragment tracks. Geochim. Cosmochim. Acta 28 (10−11), 1705–1712.
Fleischer, R.L., Price, P.B., Walker, R.M., 1975. Nuclear Tracks in Solids. University of California Press (605 pp).
Galbraith, R.F., 2005. Statistics for Fission Track Analysis. Interdisciplinary Statistics Series. Chapman & Hall/CRC Taylor & Francis Group, Boca Raton, FL, United States (USA) (219 pp).
Galbraith, R.F., Laslett, G.M., 1993. Statistical models for mixed fission track ages. Nuclear Tracks Radiat. Measure. 21 (4), 459–470.
Gleadow, A.J.W., 1981. Fission-track dating methods: what are the real alternatives? Nuclear Tracks Radiation Measure. 5 (1–2), 3–14.
Gleadow, A.J.W., Duddy, I.R., 1981. A natural long-term track annealing experiment for apatite. Nuclear Tracks 5 (1–2), 169–174.
Gleadow, A., Lovering, J., 1978. Thermal history of granitic rocks from western Victoria: A fission-track dating study. J. Geol. Soc. Aust. 25 (5–6), 323–340.
Gleadow, A.J.W., Duddy, I.R., Green, P.F., Hegarty, K.A., 1986a. Fission track lengths in the apatite annealing zone and the interpretation of mixed ages. Earth Planet. Sci. Lett. 78 (2–3), 245–254.
Gleadow, A.J.W., Duddy, I.R., Green, P.F., Lovering, J.F., 1986b. Confined fission track lengths in apatite: A diagnostic tool for thermal history analysis. Contrib. Mineral. Petrol. 94 (4), 405–415.
Gleadow, A.J.W., Belton, D.X., Kohn, B.P., Brown, R.W., 2002. Fission track dating of phosphate minerals and the thermochronology of apatite. Rev. Mineral. Geochem. 48, 579–630.
Gleadow, A.J.W., Gleadow, S.J., Belton, D.X., Kohn, B.P., Krochmal, M.S., 2009. Coincidence mapping – a key strategy for the automatic counting of fission tracks in natural minerals. Geol. Soc. Lond., Spec. Publ. 324 (1), 25–36.
Gleadow, A., Harrison, M., Kohn, B., Lugo-Zazueta, R., Phillips, D., 2015. The fish Canyon Tuff: A new look at an old low-temperature thermochronology standard. Earth Planet. Sci. Lett. 424, 95–108.
Gleadow, A.J.W., Kohn, B.P., Seiler, C., 2019. The future of fission track thermochronology. In: Malusà, M., Fitzgerald, P. (Eds.), Fission-Track Thermochronology and its Application to Geology, Springer Textbooks in Earth Sciences, Geography and Environment. Springer, Cham, pp. 77–92.
Glorie, S., et al., 2017. Thermal history and differential exhumation across the Eastern Musgrave Province, South Australia: Insights from low-temperature thermochronology. Tectonophysics 703, 23–41.
Green, P.F., 1988. The relationship between track shortening and fission track age reduction in apatite: combined influences of inherent instability, annealing anisotropy, length bias and system calibration. Earth Planet. Sci. Lett. 89 (3–4), 335–352.
Green, P.F., Laslett, G.M., Duddy, I.R., Gleadow, A.J.W., Tingate, P.R., 1986. Thermal annealing of fission tracks in apatite: 1. A qualitative description. Chem. Geol. Isotope Geosci. Sect. 59 (4), 237–253.
Guedes, S., et al., 2003. Spontaneous-fission decay constant of U-238 measured by nuclear track techniques without neutron irradiation. J. Radioanal. Nucl. Chem. 258 (1), 117–122.
Guillong, M., Günther, D., 2002. Effect of particle size distribution on ICP-induced elemental fractionation in laser ablation-inductively coupled plasma-mass spectrometry. J. Anal. At. Spectrom. 17 (8), 831–837.
Hasebe, N., Barbarand, J., Jarvis, K., Carter, A., Hurford, A.J., 2004. Apatite fission-track chronometry using laser ablation ICP-MS. Chem. Geol. 207 (3–4), 135–145.
Hasebe, N., Carter, A., Hurford, A.J., Arai, S., 2009. The effect of chemical etching on LA–ICP-MS analysis in determining uranium concentration for fission-track chronometry. Geol. Soc. Lond., Spec. Publ. 324 (1), 37–46.
Hasebe, N., Tamura, A., Arai, S., 2013. Zeta equivalent fission-track dating using LA-ICP-MS and examples with simultaneous U–Pb dating. Island Arc 22 (3), 280–291.
Holden, N.E., Hoffman, D.C., 2000. Spontaneous fission half-lives for ground-state nuclide (Technical report). Pure Appl. Chem. 72 (8), 1525–1562.
Hurford, A.J., 1990. Standardization of fission track dating calibration: Recommendation by the Fission Track Working Group of the I.U.G.S. Subcommission Geochronol. Chem. Geol. Isotope Geosci. Sect. 80 (2), 171–178.
Hurford, A.J., Green, P.F., 1982. A users' guide to fission track dating calibration. Earth Planet. Sci. Lett. 59 (2), 343–354.
Hurford, A.J., Green, P.F., 1983. The zeta age calibration of fission-track dating. Isot. Geosci. 1 (4), 285–317.
Hurford, A.J., Hammerschmidt, K., 1985. ^{40}Ar/^{39}Ar and K/Ar dating of the Bishop and fish Canyon tuffs: Calibration ages for fission-track dating standards. Chem. Geol. Isotope Geosci. Sect. 58 (1–2), 23–32.
Ito, K., Hasebe, N., 2011. Fission-track dating of Quaternary volcanic glass by stepwise etching. Radiat. Meas. 46 (2), 176–182.
Iwano, H., Danhara, T., 1998. A re-investigation of the geometry factors for fission-track dating of apatite, sphene and zircon. In: Van Den Haute, P., De Corte, F. (Eds.), Advances in Fission-Track Geochronology. Kluwer Academic Publishing, Netherlands, pp. 47–66.
Iwano, H., Kasuya, M., Danhara, T., Tamashita, T., Tagami, T., 1993. Track counting efficiency and unetchable track range in apatite. Nuclear Tracks Radiation Measure. 21 (4), 513–517.
Jaffey, A., Flynn, K., Glendenin, L., Bentley, W.T., Essling, A., 1971. Precision measurement of half-lives and specific activities of U 235 and U 238. Physical Review C 4 (5), 1889.
Jochum, K., Stoll, B., Herwig, K., Willbold, M., 2007. Validation of LA-ICP-MS trace element analysis of geological glasses using a new solid-state 193 nm Nd: YAG laser and matrix-matched calibration. J. Anal. At. Spectrom. 22 (2), 112–121.
Jolivet, M., Dempster, T., Cox, R., 2003. Répartition de l'uranium et du thorium dans les apatites: implications pour la thermochronologie U-Th/he. Compt. Rendus Geosci. 335 (12), 899–906.
Jonckheere, R., Van den Haute, P., 2002. On the efficiency of fission-track counts in an internal and external apatite surface and in a muscovite external detector. Radiat. Meas. 35 (1), 29–40.
Kelley, C.T., 2003. Solving nonlinear equations with Newton's method. Society for Industrial and Applied Mathematics, 2003 Jan 1.
Ketcham, R.A., Carter, A., Donelick, R.A., Barbarand, J., Hurford, A.J., 2007. Improved modeling of fission-track annealing in apatite. Am. Mineral. 92 (5–6), 799–810.
Kohn, B.P., et al., 2009. A reappraisal of low-temperature thermochronology of the eastern Fennoscandia Shield and radiation-enhanced apatite fission-track annealing. Geol. Soc. Lond., Spec. Publ. 324 (1), 193–216.
Kohn, B., Chung, L., Gleadow, A., 2019. Chapter 2. Fission-track analysis: Field collection, sample preparation and data acquisition. In: Malusà, M., Fitzgerald, P. (Eds.), Fission-Track Thermochronology and its Application to Geology, Springer Textbooks in Earth Sciences, Geography and Environment. Springer, Cham, pp. 25–88.
Krishnaswami, S., Lal, D., Prabhu, N., Macdougall, D., 1974. Characteristics of fission tracks in zircon: applications to geochronology and cosmology. Earth Planet. Sci. Lett. 22 (1), 51–59.
Laslett, G.M., Green, P.F., Duddy, I.R., Gleadow, A.J.W., 1987. Thermal annealing of fission tracks in apatite; 2. A quantitative analysis. Chem. Geol. Isotope Geosci. Sect. 65 (1), 1–13.
Li, G., et al., 2016. Synorogenic morphotectonic evolution of the Gangdese batholith, South Tibet: Insights from low-temperature thermochronology. Geochem. Geophys. Geosyst. 17 (1), 101–112.
Lorencak, M., Kohn, B.P., Osadetz, K.G., Gleadow, A.J.W., 2004. Combined apatite fission track and (U-Th)/he thermochronometry in a slowly cooled terrane: results from a 3440-m-deep drill hole in the southern Canadian Shield. Earth Planet. Sci. Lett. 227 (1–2), 87–104.
McDougall, I., Wellman, P., 2011. Calibration of GA1550 biotite standard for K/Ar and 40Ar/39Ar dating. Chem. Geol. 280 (1–2), 19–25.
McDowell, F.W., McIntosh, W.C., Farley, K.A., 2005. A precise ^{40}Ar/^{39}Ar reference age for the Durango apatite (U-Th)/he and fission-track dating standard. Chem. Geol. 214 (3–4), 249–263.
McMillan, M.F., Boone, S.C., Kohn, B.P., Gleadow, A.J., Chindandali, P.R., 2022. Development of the Nyika Plateau, Malawi: A Long Lived Paleo-Surface or a Contemporary Feature of the East African Rift? Geochem. Geophys. Geosyst. 23 (8).
Morrison, C., Lambert, D., Morrison, R., Ahlers, W., Nicholls, I., 1995. Laser ablation-inductively coupled plasma-mass spectrometry: an investigation of elemental responses and matrix effects in the analysis of geostandard materials. Chem. Geol. 119 (1–4), 13–29.
Noda, A., Danhara, T., Iwano, H., Hirata, T., 2017. LA-ICP-MS U–Pb and fission-track ages of felsic tuff beds of the Takikubo Formation, Izumi Group in the Kan-onji district, eastern Shikoku, southwestern Japan. Bull. Geol. Surv. Jpn 68 (3), 119–130.
Paton, C., Hellstrom, J., Paul, B., Woodhead, J., Hergt, J., 2011. Iolite: Freeware for the visualisation and processing of mass spectrometric data. J. Anal. At. Spectrom. 26 (12), 2508–2518.
Phillips, D., Matchan, E.L., 2013. Ultra-high precision 40Ar/39Ar ages for fish Canyon Tuff and Alder Creek Rhyolite sanidine: New dating standards required? Geochim. Cosmochim. Acta 121 (0), 229–239.
Reed, W., 1992a. Certificate of Analysis: Standard Reference Materials 610–611. National Institute of Standards and Technology.
Reed, W., 1992b. Certificate of Analysis: Standard Reference Materials 612–613. National Institute of Standards and Technology.
Reed, W., 1992c. Certificate of Analysis: Standard Reference Materials 614–615. National Institute of Standards and Technology.
Reiners, P.W., Thomson, S.N., McPhillips, D., Donelick, R.A., Roering, J.J., 2007. Wildfire thermochronology and the fate and transport of apatite in hillslope and fluvial environments. J. Geophys. Res. 112, F04001.
Rolland, Y., Bernet, M., van Der Beek, P., Gautheron, C., Duclaux, G., Bascou, J., Balvay, M., Héraudet, L., Sue, C., Ménot, R.P., 2019. Late Paleozoic ice age glaciers shaped East Antarctica landscape. Earth Planet. Sci. Lett. 506, 123–133.

Seiler, C., 2009. Structural and Thermal Evolution of the Gulf Extensional Province in Baja California, Mexico: Implications for Neogene Rifting and Opening of the Gulf of California. PhD Thesis,. The University of Melbourne, Melbourne (307 pp).
Soares, C.J., et al., 2013. Further investigation of the initial fission-track length and geometry factor in apatite fission-track thermochronology. Am. Mineral. 98 (8–9), 1381–1392.
Soares, C.J., et al., 2014. Novel calibration for LA-ICP-MS-based fission-track thermochronology. Phys. Chem. Miner. 41 (1), 65–73.
Soares, C.J., Mertz-Kraus, R., Guedes, S., Stockli, D.F., Zack, T., 2015. Characterisation of Apatites as potential Uranium Reference Materials for Fission-track Dating by LA-ICP-MS. Geostand. Geoanal. Res. 39 (3), 305–313.
Steiger, R.H., Jaeger, E., 1977. Subcommission on geochronology: Convention on the use of decay constants in geo- and cosmochronology. Earth Planet. Sci. Lett. 36 (3), 359–362.
Sueoka, S., et al., 2012. Denudation history of the Kiso Range, Central Japan, and its tectonic implications: Constraints from low-temperature thermochronology. Island Arc 21 (1), 32–52.
Sun, Y., Chen, Z., Boone, S.C., Zhong, F., Tao, W., 2021. Exhumation history and preservation of the Changjiang uranium ore field, South China, revealed by (U-Th)/He and fission track thermochronology. Ore Geol. Rev. 133, 104101.
Suzuki, K., 1988. Heterogeneous distribution of uranium within zircon grains: Implications for fission-track dating. J. Geol. Soc. Jpn. 94 (1), 1–10.
Svojtka, M., Kosler, J., 2002. Fission-track dating of zircon by laser ablation ICPMS, Goldschmidt. Geochim. Cosmochim. Acta A756.
Tian, Y., Kohn, B.P., Gleadow, A.J., Hu, S., 2014. A thermochronological perspective on the morphotectonic evolution of the southeastern Tibetan Plateau. J. Geophys. Res. Solid Earth 119 (1), 676–698.
Togliatti, V., 1965. Distribuzioni dei ranges e distribuzione angolare delle trace di fissionefossili di 235U in mica. Boll. Geofis. Teor. Appl. 7, 326–335.
Vermeesch, P., 2017. Statistics for LA-ICP-MS based fission track dating. Chem. Geol. 456, 19–27.
Wagner, G., 1979. Correction and interpretation of fission track ages, Lectures in isotope geology. Springer 170–177.
Wagner, G., Van Den Haute, P., 1992. Fission-Track Dating. Solid Earth Sciences Library, vol. 6. Kluwer, Dordrecht, p. 285.
Yoshioka, T., Tsuruta, T., Iwano, H., Danhara, T., 2005. Spontaneous fission decay constant of 238 U determined by SSNTD method using CR-39 and DAP plates. Nucl. Instrument. Meth. Phys. Res. Sect. A Accel. Spectrom. Detect. Assoc. Equip. 555 (1), 386–395.